

Relative sea-level change, climate, and sequence boundaries: insights from the Kimmeridgian to Berriasian platform carbonates of Mount Salève (E France)

Telm Bover-Arnal · André Strasser

Received: 12 January 2012 / Accepted: 8 June 2012 / Published online: 22 July 2012
© Springer-Verlag 2012

Abstract The present study analyses the stratal architecture of the Late Jurassic (Kimmeridgian) to Early Cretaceous (Berriasian) sedimentary succession of Mount Salève (E France), and four Berriasian stratigraphic intervals containing four sequence-boundary zones reflecting lowering trends of the relative sea-level evolution. Massive Kimmeridgian limestones characterized by the presence of colonial corals appear to be stacked in an aggrading pattern. These non-bedded thick deposits, which are interpreted to have formed in balance between relative sea-level rise and carbonate accumulation, suggest a keep-up transgressive system. Above, well-bedded Tithonian-to-Berriasian peritidal carbonates reflect a general loss of accommodation. These strata are interpreted as a highstand normal-regressive unit. During the early phase of this major normal regression, the vertical repetition of upper intertidal/lower supratidal lithofacies indicates an aggrading depositional system. This is in agreement with an early stage of a highstand phase of relative sea level. The Berriasian sequence-boundary zones investigated (up to 4 m thick) developed under different climatic conditions and correspond to higher-frequency, forced- and normal-regressive stages of relative sea-level changes. According to the classical sequence-stratigraphic principles, these sequence-boundary zones comprise more than one candidate surface for a sequence boundary. Three sequence-boundary zones studied in Early Berriasian rocks lack coarse siliciclastic grains, contain a calcrete crust, as well

as marly levels with higher abundances of illite with respect to kaolinite, and exhibit fossilized algal-microbial laminites with desiccation polygons. These sedimentary features are consistent with more arid conditions. A sequence-boundary zone interpreted for the Late Berriasian corresponds to a coal horizon. The strata above and below this coal contain abundant quartz and marly intervals with a higher kaolinite content when compared to the illite content. Accordingly, this Late Berriasian sequence-boundary zone was formed under a more humid climate. The major transgressive–regressive cycle of relative sea level identified and the climate change from more arid to more humid conditions recognized during the Late Berriasian have been reported also from other European basins. Therefore, the Kimmeridgian to Berriasian carbonate succession of Mount Salève reflects major oceanographic and climatic changes affecting the northern margin of the Alpine Tethys ocean and thus constitutes a reliable comparative example for the analysis of other coeval sedimentary records. In addition, the stratigraphic intervals including sequence-boundary zones characterized in this study constitute potential outcrop analogues for sequence-boundary reflectors mapped on seismic profiles of subsurface peritidal carbonate successions. The detailed sedimentological analyses provided here highlight that on occasions the classical principles of sequence stratigraphy developed on seismic data are difficult to apply in outcrop. A sequence-boundary reflector when seen in outcrop may present successive subaerial exposure surfaces, which formed due to high-frequency sea-level changes that were superimposed on the longer-term trend of relative sea-level fall.

T. Bover-Arnal (✉) · A. Strasser
Département de Géosciences, Université de Fribourg,
Chemin du Musée 6, 1700 Fribourg, Switzerland
e-mail: telm.boverarnal@unifr.ch

Keywords Berriasian · Sequence stratigraphy · Carbonate platform · Sea-level change · Palaeoclimate · France

Introduction

The vast subtropical-to-tropical Mesozoic carbonate platforms flourishing throughout the margins of the Tethyan and proto-Atlantic realms were reliable recorders of low- and high-frequency changes in relative sea level (e.g., Pasquier and Strasser 1997; Bádenas et al. 2004; Colombié and Rameil 2007). On the flat-lying platform tops (e.g., Borgomano 2000; Booler and Tucker 2002; Bover-Arnal et al. 2009) or on gently sloping proximal ramps (e.g., Van Buchem et al. 2002; Aurell and Bádenas 2004; Bover-Arnal et al. 2010), even low-amplitude, metric shifts of relative sea level were recorded and are evidenced by repeated subaerial exposure or maximum regressive surfaces followed by transgressive intervals.

Regional-to-global relative sea-level fluctuations are mainly controlled by glacial and thermal eustasy, thermal and tectonic subsidence, uplift processes, and sediment supply to the basins. The complex interplay between these mechanisms normally results in a hierarchical stacking of the strata that reflects different orders of depositional cyclicity (e.g., Strasser et al. 2006; Spence and Tucker 2007; Catuneanu et al. 2009). The cyclic variations of controlling parameters are highlighted by the repetition of particular lithofacies successions at distinct scales of space and time. The analysis of the different orders of cyclicity in the rock record by means of sequence- and cyclostratigraphy is of importance to interpret the stratigraphic packaging within a basin, to discriminate between autocyclic and allocyclic processes that were responsible for creating the observed sedimentary sequences, and to quantify rates and amplitudes of the controlling processes.

The Berriasian (Early Cretaceous) exposures on the north-western, almost vertical face of Mount Salève (E France), are a well-studied example of a carbonate sedimentary succession that was controlled by different orders of relative sea-level variations (Strasser 1988, 1994; Strasser and Hillgärtner 1998; Hillgärtner 1999; Strasser et al. 1999, 2000, 2004; Hillgärtner and Strasser 2003). According to Strasser and Hillgärtner (1998), three different orders of relative sea-level change, which were at least partly governed by orbital forcing, can be interpreted from these platform carbonates. The higher-frequency sea-level fluctuations identified were in tune with the 100- and 400-kyr eccentricity cycles, while the lower-order sea-level changes are correlatable with the Berriasian sequences reported for the European basins by Hardenbol et al. (1998). Accordingly, the Berriasian section of Mount Salève contains 8 sequence boundaries that mark significant long-term falls of relative sea level (Strasser and Hillgärtner 1998). In addition, Strasser (1988) linked smaller-scale, elementary sequences interpreted from the same sedimentary succession to the 20-kyr precession cycle.

Sequence boundaries are prominent stratigraphic elements that subdivide the sedimentary record into genetic units. The sedimentary expression of a sequence boundary related to relative sea-level fall can be very variable depending on the nature and topography of the underlying strata, the time involved in its formation, the climate, the depositional space available, the biotic activity, the physical and chemical oceanographic conditions, the diagenetic processes, the type of sediment supply, and the rates of sedimentation. Four different types of sequence boundary can be formed during regressive stages of relative sea level: the subaerial unconformity, the correlative conformity, the regressive surface of marine erosion, and the maximum regressive surface (Catuneanu et al. 2009). If these surfaces are reworked during the subsequent transgression, the sequence boundary is replaced by a transgressive ravinement surface.

Sequence boundaries Be1, Be2, Be4, and Be8 of Mount Salève (Strasser and Hillgärtner 1998) and the strata below and above these diagnostic surfaces developed under distinct environmental conditions during the Berriasian age. One of the aims of the present paper is to analyse these stratigraphic intervals to provide case studies illustrating distinct sedimentary expressions of a sequence boundary, that is, different reactions of the depositional environment to lowering sea level under varying, additional, controlling factors. The stratigraphic intervals examined were chosen because of their excellent exposure and because they each provide unambiguous palaeoclimatic information. The second goal of the paper is to place these Berriasian strata within a large-scale sequence-stratigraphic context comprising the whole of the Kimmeridgian to Berriasian succession that builds up the cliffs of Mount Salève.

Since the earliest days of Geology, Mount Salève has received considerable attention concerning palaeontology, stratigraphy, sedimentology, and structural geology (e.g., de Saussure 1779–1796; Joukowsky and Favre 1913; Carozzi 1955; Lombard 1967; Deville 1991; Gorin et al. 1993; Signer and Gorin 1995; Hillgärtner 1998). However, none of the published studies have tackled the aforementioned objectives.

Geographical and geological setting of the study area

Located in the Haute Savoie (E France), to the south of Geneva (Switzerland), Mount Salève rises from the surrounding plains as an elongate structural dome roughly 17 km long and 3 km wide (Fig. 1). This structure represents the Mesozoic head of a thrust-sheet that overrides the Late Oligocene–Early Miocene Molasse basin (Gorin et al. 1993). Steep cliffs at the north-western side expose a Kimmeridgian to Late Berriasian sedimentary succession

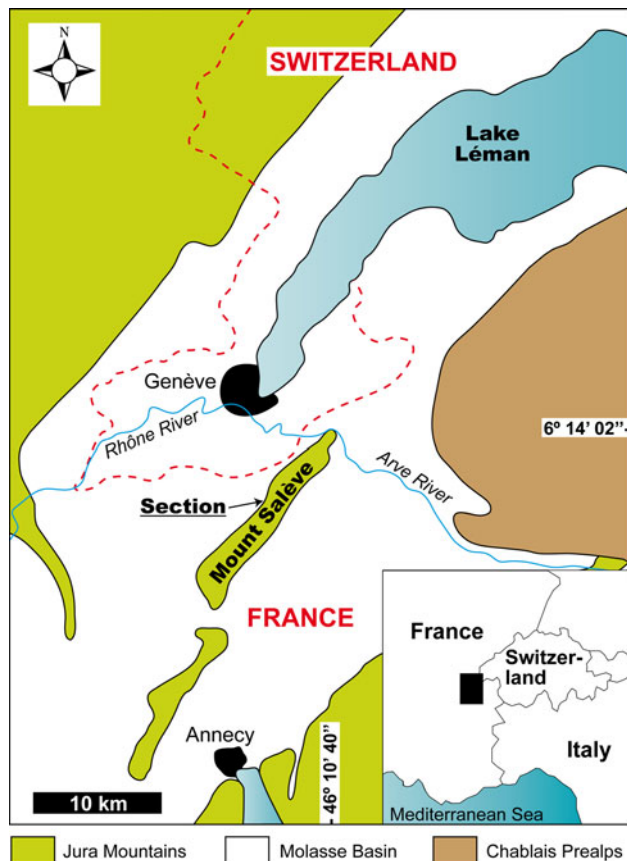


Fig. 1 Location map of the studied section in the north-western cliffs of Mount Salève in E France

composed of marine platform carbonates, which occasionally alternate with freshwater limestones (Strasser 1988; Deville 1991). The Berriasian strata analysed in this study are found in these cliff exposures (Fig. 1), along an almost vertical section that commences at the intersection between the Chavardon and Etiollets trails, follows uphill along the Etournelles trail, and ends above the Corratierie trail (see Strasser and Hillgärtner 1998).

The Late Jurassic stratigraphy of Mount Salève lacks precise dating and formal stratigraphic units (Deville 1991). Coral-bearing limestones, which belong to the “Calcaires à tertres récifaux des Etiollets” Member of the informal formation of the “Calcaires coralliens des Etiollets” (Fig. 2; Deville 1990), are of probable Kimmeridgian (-Tithonian?) age and build up the lower part of the succession. Above, limestones containing oncoids are interpreted to be equivalent to the Chailley Formation of Enay (1965) (Fig. 2) and, thus, of Tithonian age (Bernier 1984). The Berriasian succession covers a time interval of 5.3 My (according to Gradstein et al. 2004), is 154 m thick (Strasser and Hillgärtner 1998), and can be divided into 5 lithostratigraphic units with the rank of formations: Tidalites-de-Vouglans, Goldberg, Pierre-Châtel, Vions, and

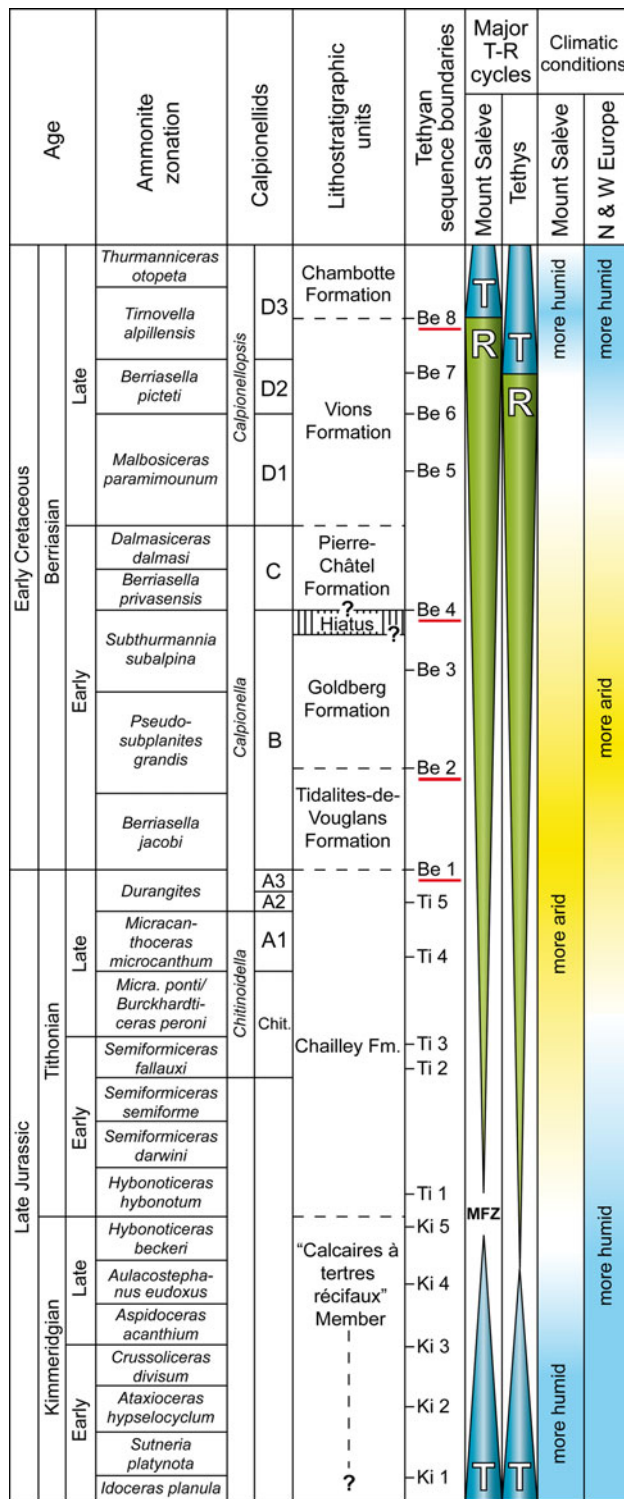
Chambotte (Fig. 2; Häfeli 1966; Steinhäuser and Lombard 1969; Bernier 1984). The age of the deposits has been calibrated by ammonite and calpionellid biostratigraphy (Le Hégarat and Remane 1968). This biostratigraphic framework is strengthened by high-resolution cyclostratigraphic analyses and the identification of 8 sequence boundaries with regional significance (Strasser and Hillgärtner 1998), which enables correlations with hemipelagic basins where more precise biostratigraphic dating is available (Hardenbol et al. 1998).

Data collection and methods

The strata below and above the sequence boundaries Be1, Be2, Be4, and Be8 of Strasser and Hillgärtner (1998) were logged and sampled for sedimentological and petrographical analyses. The beds giving rise to these sedimentary successions were labelled with letters and numbers to facilitate their detailed description. In this regard, A1–H1, A2–O2, A4–G4, and A8–V8 correspond to the strata encompassing the sequence boundaries Be1, Be2, Be4, and Be8, respectively. Microfacies were studied from 99 thin sections. Panoramic photomosaics of Mount Salève taken from the environs of the villages of Troinex (Switzerland), Veyrier (Switzerland), and Collonges-sous-Salève (France) were used for mapping, line-drawing, and the large-scale sequence-stratigraphic analysis. The sequence-stratigraphic interpretation is based on the lithofacies evolution and stacking patterns mapped during field work and observed with binoculars from a distance. The terminology used for the rock textures and the sequence-stratigraphic interpretation follows Dunham (1962) and Catuneanu et al. (2009), respectively.

Large-scale sequence-stratigraphic context

The overall stratal architecture of Mount Salève can be divided into two large-scale genetic types of deposit, which reflect major trends of the relative sea-level evolution. The first unit comprises Kimmeridgian non-bedded coral-bearing limestones, which appear to be arranged in an aggrading pattern (Figs. 3, 4a). This aggrading succession, which is up to several tens of metres thick, is interpreted as a large-scale transgressive deposit whereby increasing accommodation was continuously filled by sediment (Colombié and Strasser 2005). Above, Tithonian-to-Berriasian well-bedded peritidal carbonates (around 200 m thick; Strasser and Hillgärtner 1998; Hillgärtner 1999) reflect a decreasing rate of accommodation gain and are interpreted as highstand normal-regressive deposits (Figs. 3, 4b). According to the laterally continuous and horizontal geometries, and due to the



◀ **Fig. 2** Chronostratigraphic framework for the Kimmeridgian, Tithonian, and Berriasian of Mount Salève (E France). Modified from Strasser and Hillgärtner (1998). The sequence boundaries targeted in this study are *underlined in red*. Note that besides a small phase-lag, the major Kimmeridgian–Berriasian transgressive–regressive cycle interpreted in Mount Salève fits rather well with the one reported for the European basins (Hardenbol et al. 1998). Note also that the palaeoclimatic conditions recognized in Mount Salève are in accordance with the Kimmeridgian–Berriasian north-western European climatic trends reported in the literature (Ruffell et al. 2002). The Late Jurassic palaeoclimatic data of Mount Salève are taken from Rameil (2005). Formation boundaries are marked in *dashed lines* because their exact biostratigraphic position is not known. *MFZ* maximum-flooding zone, *T* transgressive, *R* regressive

Anatomy of sequence boundaries

Sequence boundary Be1

The stratigraphic interval analysed surrounding sequence boundary (SB) Be1 commences in the uppermost Chailley Formation (A1 in Figs. 5, 6). The top of this formation is characterized by metre-thick moderately sorted grainstones (Fig. 7a) containing peloids, micritic oncoids, other coated grains, *Andersenolina* cf. *alpina*, *Mohlerina basiliensis*, other unidentified foraminifera, and skeletal fragments of green algae, echinoids, bivalves, and gastropods. No hydrodynamic structures were recognized. Keystone vugs pointing to upper intertidal to lower supratidal conditions (Dunham 1970) appear in the uppermost part of the bed.

The upper limit of the Chailley Formation corresponds to an unconformable surface that defines the limit with the Tidalites-de-Vouglans Formation (Figs. 2, 5 and 6). This surface is overlain by decimetre-thick channelized beds, which exhibit erosional features and partly pinch out laterally (B1 in Figs. 5, 6). The channelized deposits display packstone to grainstone textures and are distinguished by the presence of black granules and pebbles, peloids, micritic oncoids, other coated grains, *Andersenolina* sp., other unidentified foraminifera, and fragments of molluscs, echinoids, serpulids, corals, and dasycladaceans. These deposits are thought to have formed in the shallow subtidal realm, influenced by currents that eroded pre-existing carbonate sands and shifted sediment lobes.

The channelized and erosive subtidal strata pass laterally and upwards into decimetre-thick beds, which exhibit a mudstone texture with mm-thin laminations (C1 and E1 in Figs. 5, 6). Locally, these levels are dolomitized. They are interpreted as algal-microbial mats that formed in low-energy upper intertidal to lower supratidal conditions (e.g., Shinn et al. 1969). Millimetre-to-centimetre-thick horizons of sand-sized moulds of skeletal fragments (Fig. 7b) are interpreted as storm deposits on the tidal flat. Black granules and pebbles (Fig. 7c), other lithoclasts, mud pebbles, and mud drapes, as

absence of step-like structures (Fig. 3), the Tithonian-to-Berriasian depositional profile of Mount Salève corresponded to a flat-topped platform or a low-angle homoclinal ramp. On account of the two-dimensional aspect of the outcrop, it is not possible to determine the directions of retrogradation and progradation.

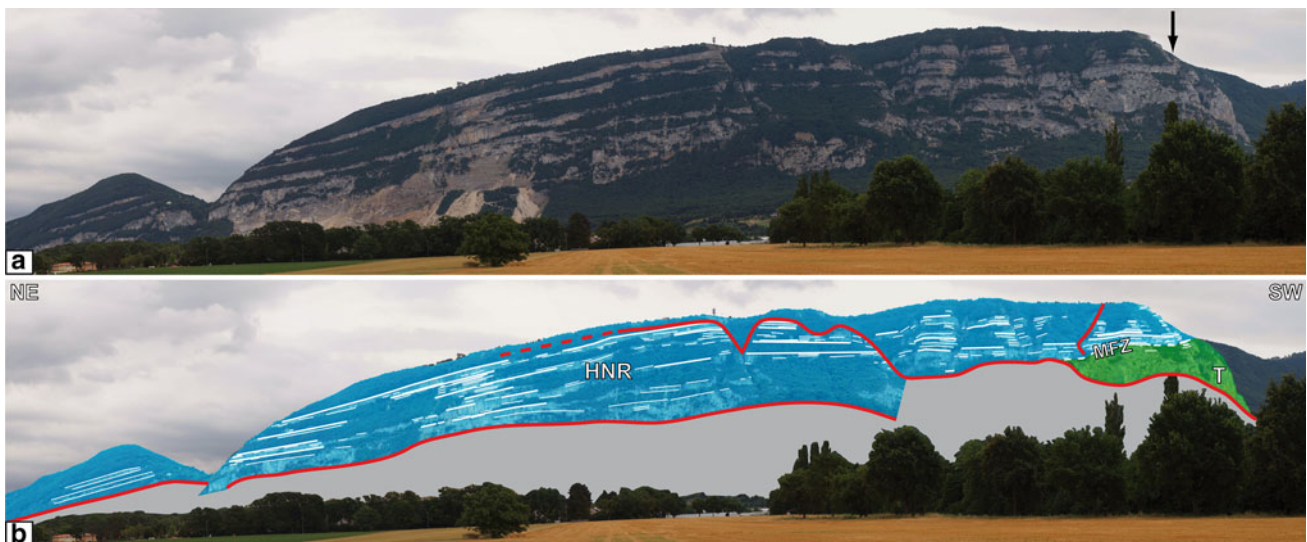


Fig. 3 Large-scale sequence-stratigraphic interpretation of Mount Salève. **a** Panoramic photomosaic, looking from NW. **b** Sequence-stratigraphic interpretation. Red lines are faults; the grey area corresponds to the north-western, vertical flank of an anticline.

HNR highstand normal-regressive deposits, *T* transgressive deposits, *MFZ* maximum-flooding zone. Arrow shows position of studied section

well as ripple structures (Fig. 7d), are also common in these deposits, pointing to reworking and tidal influence. Black pebbles and granules are furthermore indicative of nearby subaerial emergence (Strasser and Davaud 1983). Centimetre-thick beds with a wackestone texture are locally found intercalated between the algal-microbial mat layers (D1 in Figs. 5, 6). These deposits contain black granules and pebbles, miliolids, *Andersenolina* sp., other unidentified foraminifera, ostracodes, molluscs, dasycladaceans, and charcoaled fragments of conifers (Fig. 7e). They formed in a subtidal, low-energy environment.

Above, a metre-thick dolomitic limestone bed (F1 in Figs. 5, 6) exhibits a wackestone texture (Fig. 7f) and includes black granules and pebbles, porocharacean remains, ostracodes, charcoaled plant fragments, and unidentified foraminifera. Given the homogeneous high population density of porocharacean gyrogonites and stems, this bed is seen as representing a brackish-water environment (e.g., Climent-Domènech et al. 2009). Decimetre-thick low-energy wackestones dominated by miliolids, reworked porocharacean gyrogonites and fragments of bivalves, gastropods, and dasycladaceans then indicate a marine transgression (G1 in Fig. 5). Upwards in the succession, the wackestone beds evolve into metre-thick massive dolomitic limestones (H1 in Fig. 5). The base of these deposits comprises mudstones and brecciated fabrics with miliolids, other unidentified foraminifera, micritic oncoids, and fragments of green algae. Above, poorly sorted grainstones with peloids, micritic oncoids, ooids, unidentified foraminifera and fragments of echinoids, dasycladaceans, and molluscs dominate.

Sequence boundary Be2

The lower part of the stratigraphic interval that comprises SB Be2 corresponds to decimetre-thick beds (Fig. 4b) with wackestone texture containing peloids, oncoids, and fragments of molluscs and green algae (A2–C2 in Fig. 8). These low-energy subtidal lithofacies evolve upwards in the succession to decimetre-thick mudstones (D2–E2 in Figs. 8, 9) exhibiting desiccation cracks (Fig. 10a) and represent the low-energy intertidal to supratidal realm (e.g., Hardie 1977). The top of bed E2 with the well-developed desiccation polygons corresponds to the top of the Tidalites-de-Vouglans Formation.

Above, a marly interval of 5 cm (F2 in Figs. 8, 9) is followed by a 45-cm-thick bed of very well-sorted grainstone (G2 in Figs. 8, 9 and 10b), which displays keystone vugs (Fig. 10c) and bi-directional cross-bedding structures. It contains black granules and pebbles, other lithoclasts, micritized ooids, and fragments of bivalves and gastropods. The bed is partially broken into blocks, and the fractures that delimit the different blocks are filled with breccia/conglomerate deposits (Fig. 10d) made up of black granules and pebbles and other sand- to cobble-sized lithoclasts. This bed is interpreted as a tidally influenced ooid sand sheet that developed a beach on its top, as indicated by the keystone vugs. Subsequent rapid cementation turned it into beachrock, which probably was then undercut by waves, fractured, and dismantled into blocks (e.g., Strasser et al. 1989). The marly interval is rich in greenish illite, which typically forms in the intertidal realm (Deconinck and Strasser 1987).



Fig. 4 Field photographs of the Kimmeridgian–Berriasian sedimentary succession of Mount Salève. **a** Large-scale sequence-stratigraphic framework of Mount Salève. Note how massive, thick, non-bedded carbonates (Kimmeridgian, below) interpreted as transgressive deposits are separated by a maximum-flooding zone from well-bedded limestones (Tithonian–Berriasian, above), which are regarded as a highstand normal-regressive genetic type of deposit. *HNR* highstand normal-regressive deposits, *T* transgressive deposits, *MFZ* maximum-flooding zone. *Arrow* shows position of studied section.

Houses at the *bottom-left corner* for scale. **b** Outcrop view of the well-bedded highstand normal-regressive Berriasian strata of Mount Salève. The position of the sequence boundary (SB) Be2 of Strasser and Hillgärtner (1998) that separates the Early Berriasian Tidalites-de-Vouglans Formation from the late Early–Middle Berriasian Goldberg Formation is outlined in red. Note how the beds of the Tidalites-de-Vouglans Formation become thinner close to the sequence boundary, reflecting a loss of accommodation

The grainstone bed is overlain by a calcrete crust (up to 4 cm thick), which indicates long-lasting subaerial exposure (H2 in Figs. 8, 9, and 10e; e.g., James 1972; Robbin and Stipp 1979). The sedimentary succession continues with a centimetre-thick marly level followed by a decimetre-thick breccia/conglomerate (I2 in Figs. 8, 9, and 10e) with poorly sorted, subangular to subrounded clasts

ranging from 1 to 30 cm in diameter. The clasts display at least three different lithologies: (1) a very well-sorted grainstone with micritized ooids and fragments of molluscs corresponding to bed G2, (2) a black oolite, and (3) a wackestone to packstone with peloids, oncoids, and fragments of bivalves and gastropods. This breccia/conglomerate is interpreted to have formed in a high-energy

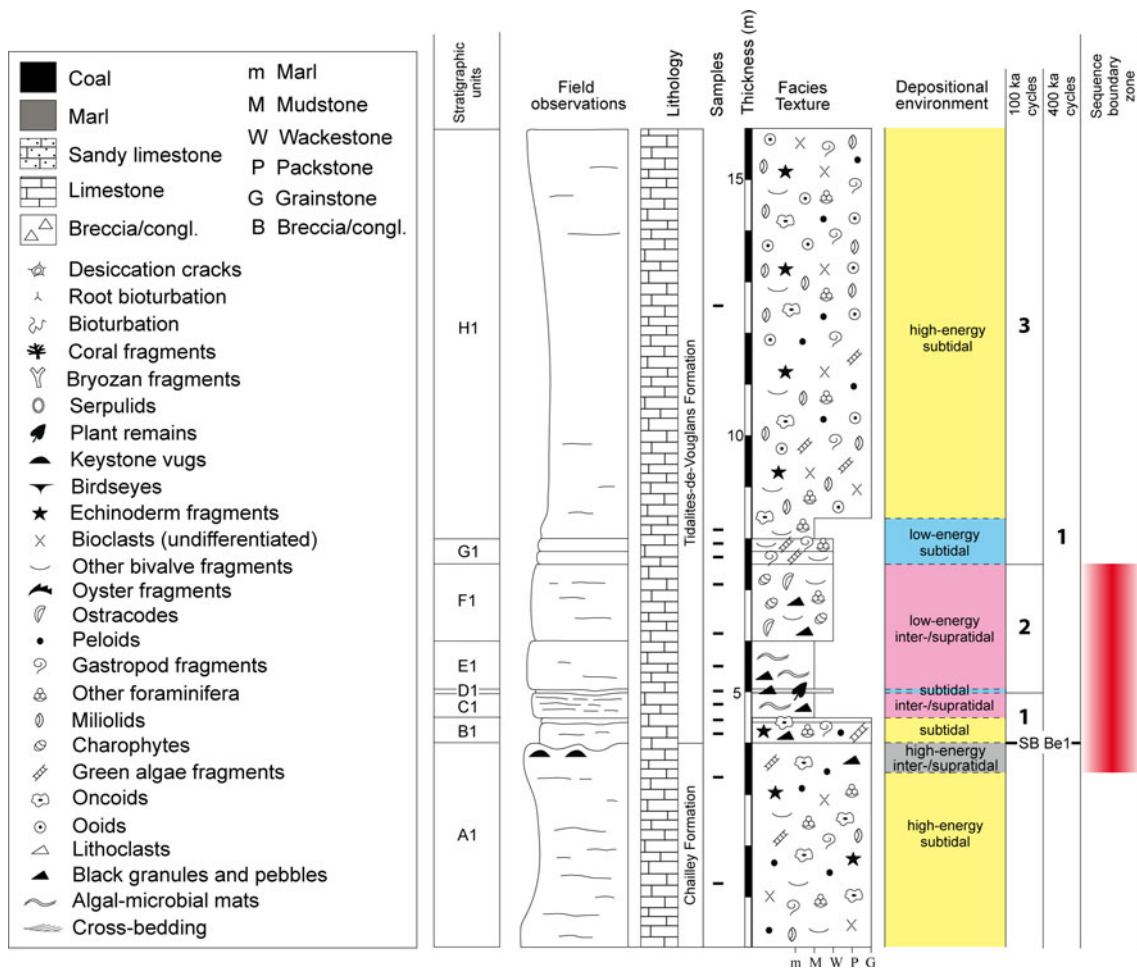


Fig. 5 Measured log and interpretation of the stratigraphic interval below and above sequence boundary (SB) Be 1. Cyclostratigraphic interpretation according to Strasser and Hillgärtner (1998)

inter-to-supratidal beach environment, reworking previously cemented sediment of different origins (e.g., El-Sayed 1999; Stephenson and Naylor 2011).

The breccia/conglomerate passes upwards into a wackestone of 35 cm (J2 in Figs. 8, 9) with black granules and pebbles, other lithoclasts, peloids, ooids, miliolids, other unidentified foraminifera, and fragments of molluscs and dasycladaceans. Above this wackestone, a centimetre-thick marly interval (K2 in Figs. 8, 9) rich in green illite (Deconinck and Strasser 1987) is followed by a coarsening-upwards mudstone to well-sorted, bi-directionally cross-bedded grainstone containing keystone vugs, mud pebbles, peloids, ooids, miliolids, and fragments of echinoids, molluscs, and green algae (L2 in Figs. 8, 9, and 10f). The top of this high-energy, tidally influenced deposit is erosive and overlain by a poorly sorted breccia/conglomerate (M2 in Figs. 8, 9 and 10f) with clasts up to 30 cm in diameter. The clast lithology corresponds to the one of bed L2 below. Above, a metre-thick massive packstone to grainstone bed (N2–O2 in Figs. 8, 9) containing black granules and

pebbles, peloids, ooids, oncoids, miliolids, other unidentified foraminifera, and skeletal fragments of echinoids, bivalves, gastropods, and dasycladaceans is attributed to a normal-marine and subtidal environment.

Sequence boundary Be4

The interval comprising SB Be4 is located around the limit between the Goldberg and Pierre-Châtel formations (Figs. 2, 11, and 12). Wackestones (A4–B4 in Fig. 11) containing ostracodes, serpulids, and fragments of unidentified molluscs are attributed to a low-energy subtidal environment. They are followed by thinly laminated mudstones with birdseyes (Fig. 13a) and desiccation cracks (C4 and D4) representing the low-energy upper intertidal to lower supratidal zone (e.g., Hardie 1977). These are then overlain by a 50-cm-thick bed of breccia/conglomerate with a marly matrix (E4 in Figs. 11, 12). The lithoclasts, some of them blackened, have diameters of up to 30 cm and display at least two different lithologies: (1) a packstone-grainstone



Fig. 6 **a** Outcrop photograph of the strata surrounding SB Be1. **b** Interpretation of figure a. Note the unconformable nature of SB Be1 (top of stratigraphic unit A1) and how the overlying strata display

texture with lithoclasts, peloids, miliolids, *Andersenolina* sp., and fragments of molluscs, and (2) a wackestone texture with lithoclasts, porocharacean remains, peloids, and fragments of molluscs and dasycladaceans. The lithoclasts were not transported from continental to coastal settings by rivers given that their edges are mostly angular, and the lithofacies are identical to the beds found above and below the breccia/conglomerate level. Laterally, in an outcrop 200 m to the NE, individual beds that sourced the lithoclasts are still recognizable (Strasser 1994). The lithoclasts were neither eroded from a palaeocliff. If so, they would be found within the beds below and above the breccia/conglomerate horizon as well. The breccia/conglomerate thus indicates a high-energy beach setting with production of cobble-to-boulder-sized clasts

irregular bounding surfaces, suggesting erosion and channelling. Some beds pinch out laterally. A1 to F1 labels correspond to beds referred to in the text and indicated in Fig. 5; hammer = 32 cm

by erosion of pre-existing limestone beds (e.g., El-Sayed 1999; Stephenson and Naylor 2011).

Above the breccia/conglomerate, a 15-cm-thick wackestone (F4 in Fig. 11, 12, and 13b) with abundant ostracodes and porocharacean gyrogonites and thalli (Fig. 13c) is embedded between two centimetre-thick marly intervals (Fig. 11). This facies formed in a brackish-water environment (e.g., Climent-Domènech et al. 2009). The marls are rich in green illite (Deconinck and Strasser 1987). The marly layers are too thin to be washed and analysed for fossil contents. However, marls in other intervals in the Salève section have furnished porocharaceans and brackish ostracods that have been used for biostratigraphy (Mojon 1988). The overlying sharp surface corresponds to the base of the Pierre-Châtel Formation. Its lower part consists of

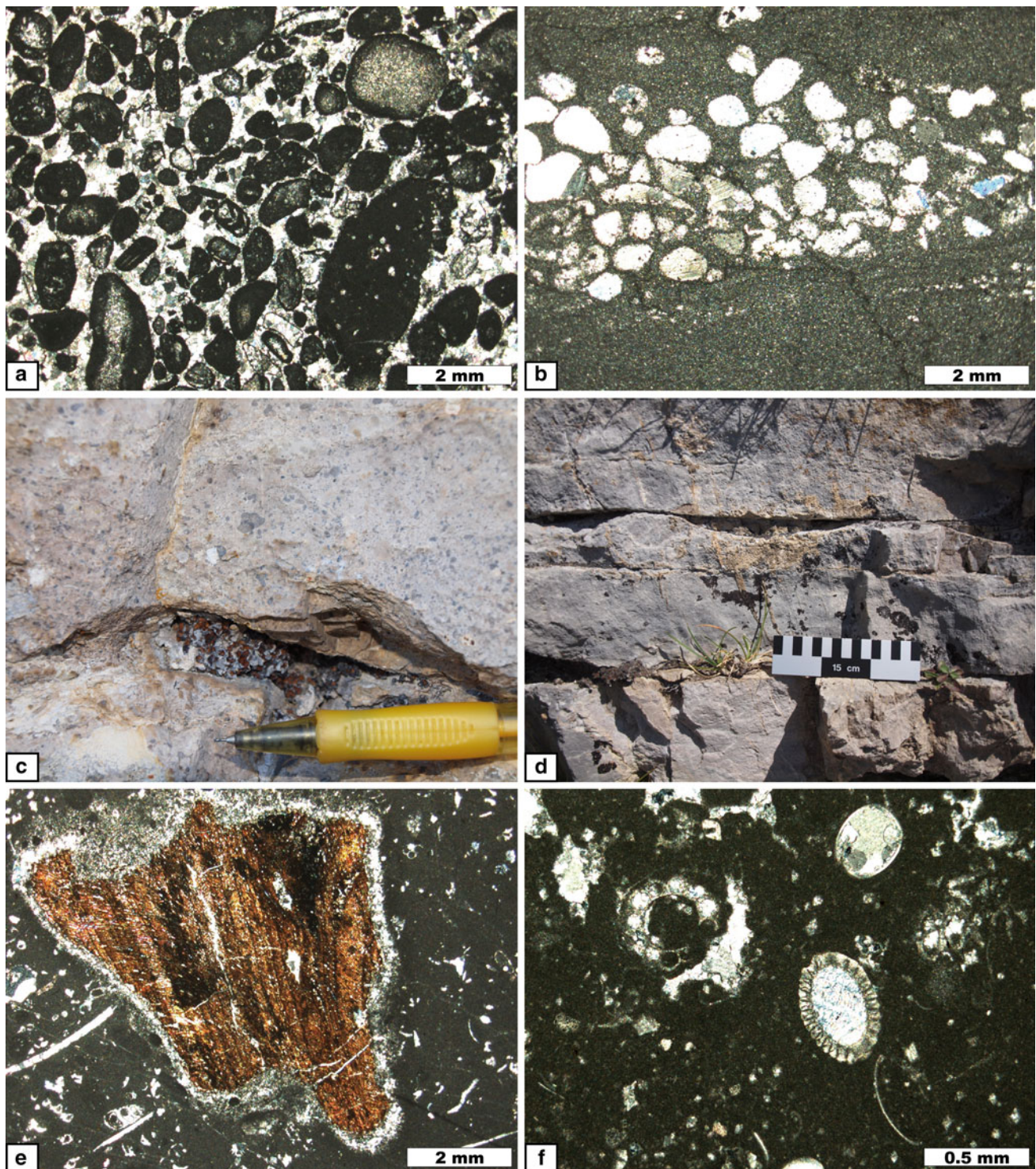
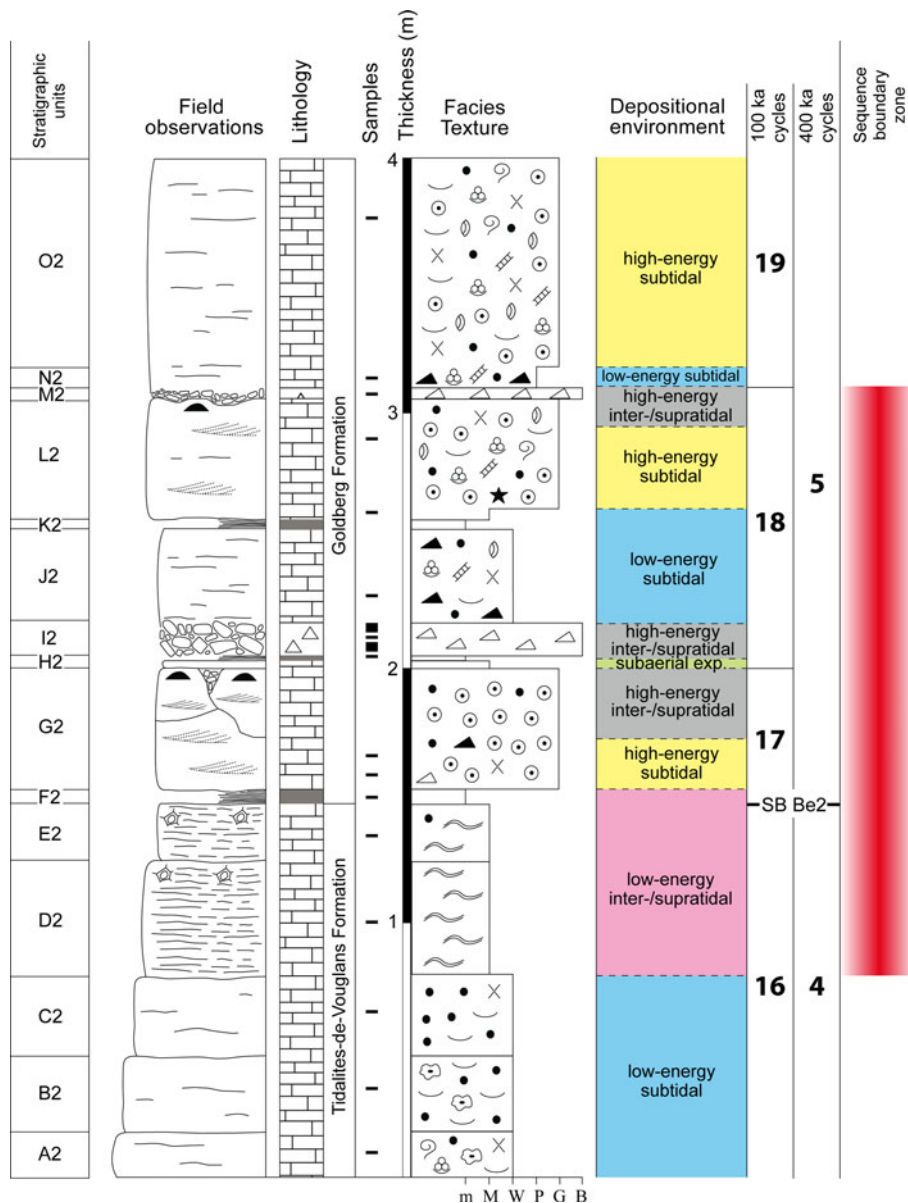


Fig. 7 Sedimentary facies around SB Be1. **a** Photomicrograph of moderately sorted grainstone microfacies characteristic of the Chailley Formation, bed A1. **b** Photomicrograph of mudstone microfacies of algal-microbial mats exhibiting a storm-lag deposit constituted by moulds of sand-sized skeletal fragments found in the lower part of the Tidalites-de-Vouglans Formation, bed E1. **c** Close-up view of black

granules and pebbles, bed C1; visible part of pen = 6.4 cm. **d** Detail of ripple structures preserved in algal-microbial mat deposits, bed C1. **e** Photomicrograph of a conifer fragment present in low-energy subtidal deposits, bed D1. **f** Photomicrograph of wackestone microfacies of brackish-water carbonates containing porocharacean stems and gyrogonites, bed F1

Fig. 8 Measured log and interpretation of the stratigraphic interval analysed surrounding sequence boundary Be 2. See Fig. 5 for legend. Cyclostratigraphic interpretation according to Strasser and Hillgärtner (1998)



thick beds of cross-bedded, moderately sorted grainstone (Fig. 13d), which indicates high-energy subtidal conditions (G4 in Figs. 11, 12, and 13b). The components present in this grainstone are peloids, ooids, other coated grains, *Andersenolina* sp., other unidentified foraminifera, fragments of coral and bryozoan colonies, echinoids, dasycladaceans, bivalves, and gastropods.

Sequence boundary Be8

The stratigraphic interval comprising SB Be8 begins in the uppermost part of the Vions Formation (Figs. 2, 14, and 15) with massive limestone beds (A8–B8 in Fig. 14) exhibiting a moderately sorted grainstone texture (Fig. 16a) and containing ooids, peloids, miliolids, *Andersenolina delphinensis*,

other unidentified foraminifera, and skeletal fragments of echinoids, molluscs, and algae such as *Clypeina parasolkani*. They point to high-energy subtidal conditions. Above these grainstones, the carbonate succession becomes siliciclastic influenced and is composed of bedded limestones with quartz sand (Fig. 16b). They have wackestone and packstone textures and contain peloids, scarce ooids, miliolids, other unidentified foraminifera, and fragments of echinoids, oysters, other unidentified bivalves, gastropods, *Clypeina* aff. *estevezi*, and other green algae (C8–J8 and L8–M8 in Figs. 14, 15). Bioturbation with *Thalassinoides* trace fossils is common. The beds display a reddish colour due to iron impregnation (Fig. 16c). A decimetre-thick marly interval is also found intercalated between these levels (K8 in Figs. 14, 15). The marls are rich in kaolinite (Hillgärtner 1999).

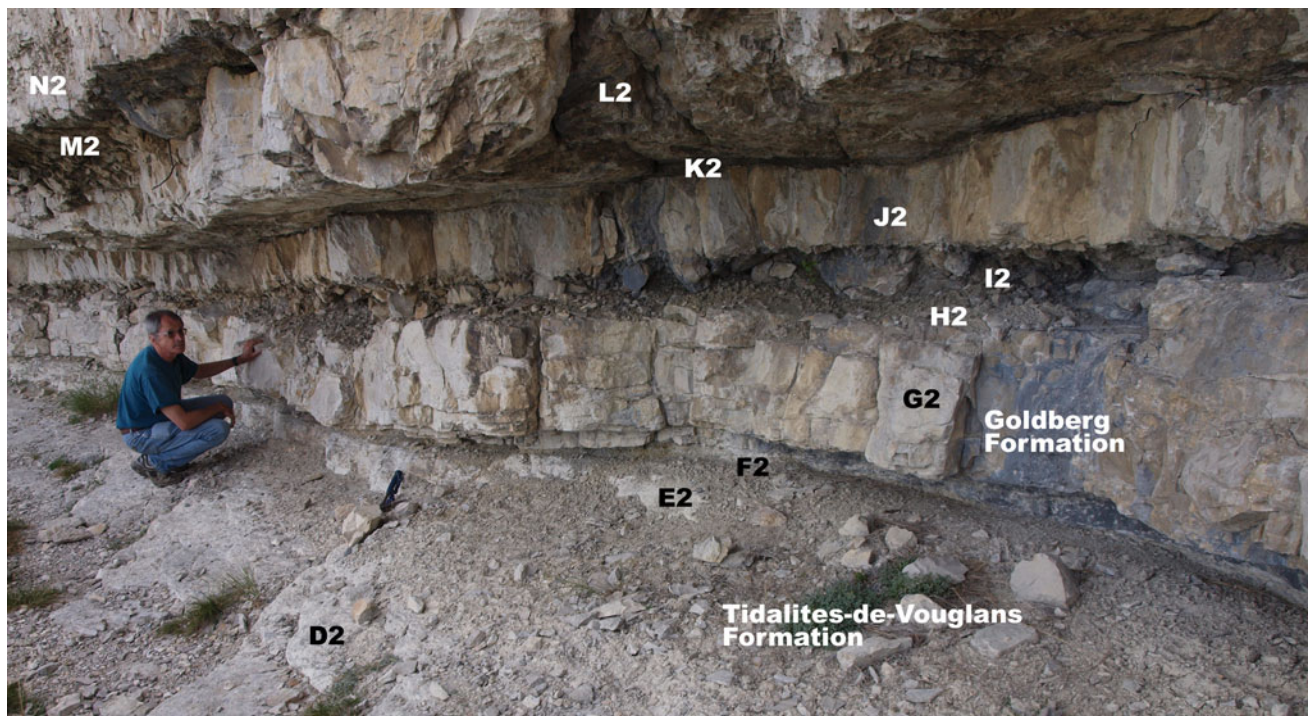


Fig. 9 Outcrop photograph of the strata surrounding SB Be2. Note how the beds are laterally continuous. D2 to N2 labels correspond to beds referred to in the text and indicated in Fig. 8

A prominent, slightly undulating surface is situated at the base of a centimetre-thick clayey coal horizon (N8 in Figs. 14, 15, and 16c). Rare root traces penetrate a few centimetres into the underlying sediment. The coal level is seen to represent a tide-influenced swamp (e.g., Shao et al. 1998) with brackish to fully marine seawater that formed on top of the bioturbated subtidal facies and that was preserved in anoxic conditions. The surface on top of bed M8 constitutes the limit between the Vions and Chambotte formations (Figs. 14, 15). Above, a 40-cm-thick bioturbated (Fig. 16d) sandy limestone bed displaying a packstone texture with peloids, miliolids, other unidentified foraminifera, and skeletal fragments of echinoids, molluscs, and dasycladaceans indicates the return to low-energy subtidal conditions (O8 in Figs. 14, 15).

Upwards in the succession, the packstone is followed by bedded sandy limestones with a moderately sorted grainstone texture, including peloids, miliolids, *Nautiloculina* cf. *brönnimanni*, other foraminifera, and fragments of echinoids, oysters, other bivalves, gastropods, and dasycladaceans (P8–T8 in Figs. 14, 15). Locally, burrow bioturbation occurs. These grainstones are succeeded by massive sandy limestones exhibiting a packstone texture, which is dominated by peloids, miliolids, other unidentified foraminifera, and fragments of oysters, other unidentified bivalves, gastropods, echinoids, and dasycladaceans (U8–V8 in Fig. 14). The facies of beds P8 to V8 indicate subtidal, normal-marine conditions.

Key fossil markers widely known from Mount Salève such as *Favreina salevensis*, *Clypeina jurassica*, *Montsalevia salevensis*, and *Hypelasma salevensis* (e.g., Joukowsky and Favre 1913; Gourrat et al. 2003) were not identified in the rocks and thin sections analysed.

Discussion

Major trends of relative sea level

In two-dimensional tectonized outcrops lacking lateral stratal terminations such as the north-western face of Mount Salève (Fig. 3), it is always risky to perform sequence-stratigraphic analyses. However, the large-scale architectural and sequence-stratigraphic interpretation of the Late Jurassic (Kimmeridgian) to Early Cretaceous (Berriasian) sedimentary succession examined is consistent with the lithofacies evolution and the stacking patterns observed.

The Kimmeridgian coral-bearing limestones of the lower part of the succession lack clear bedding planes (Figs. 3, 4a). Massive deposits of several tens of metres thick such as these Kimmeridgian rocks imply rising relative sea level and creation of depositional space, which was continuously filled by carbonate sediments. This scenario suggests a keep-up carbonate system, which can be

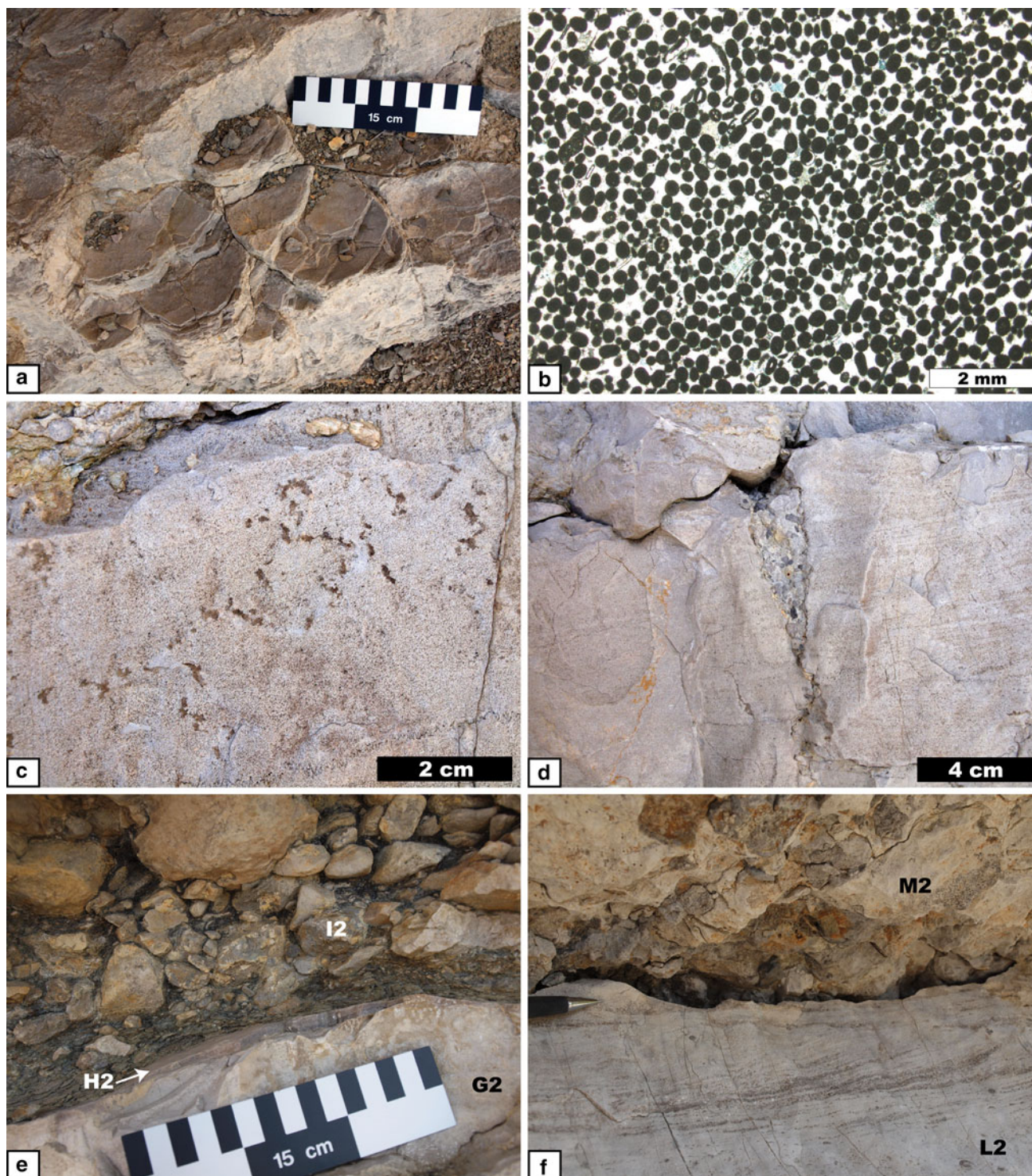
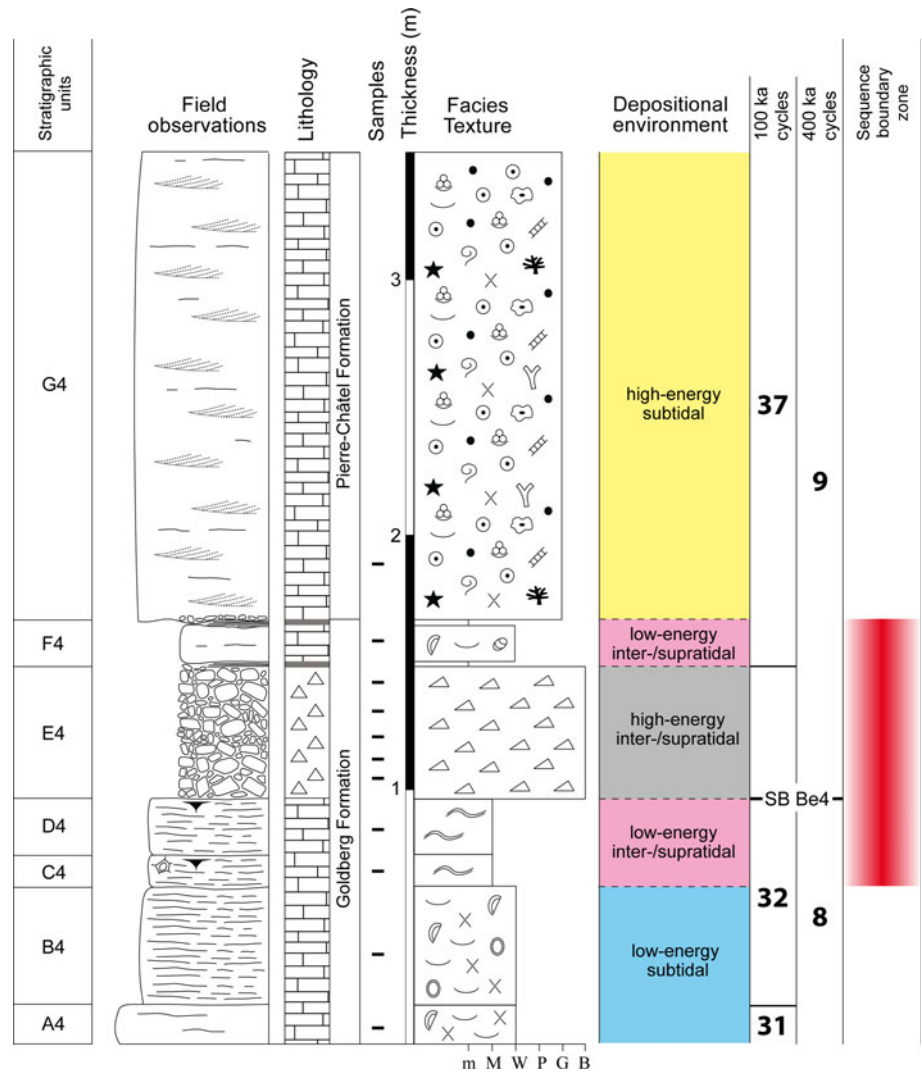


Fig. 10 Sedimentary facies around SB Be2. **a** Close-up view of polygonal desiccation cracks present at the top of the Tidalites-de-Vouglans Formation, bed E2. **b** Photomicrograph of very well-sorted grainstone of micritized ooids in the lowermost part of the Goldberg Formation, bed G2. **c** Irregularly oriented keystone vugs in the upper part of bed G2. **d** Close-up view of a fracture filled with a breccia/conglomerate deposit within the partially broken grainstone of bed

G2. **e** Detail of the calcrete laminar crust (H2) overlying bed G2. Note the presence of a marly interval followed by a poorly sorted breccia/conglomerate (I2) above the calcrete crust. **f** Close-up view of complex cross-bedding structures exhibited by the grainstone of bed L2. Note the irregular, erosive surface of the bed and the overlying breccia/conglomerate deposit (M2); visible part of pen = 2.9 cm

Fig. 11 Measured log and interpretation of the stratigraphic interval surrounding sequence boundary Be 4. See Fig. 5 for legend. Cyclostratigraphic interpretation according to Strasser and Hillgärtner (1998)



interpreted as a large-scale transgressive genetic type of deposit. On a regional scale, this interpretation is in accordance with the results of Colombié and Strasser (2005) who describe a coeval carbonate system in north-western Switzerland that kept up with relative sea-level rise.

The Tithonian-to-Berriasian deposits of the upper part of the succession exhibit well-bedded strata (Figs. 3, 4b) which, in contrast to the massive Kimmeridgian rocks, are interpreted to reflect generally low accommodation gain. The lithofacies were generated in very shallow subtidal, intertidal, and even supratidal environments (Figs. 5, 6, 7, 8, 9, 10, 11, 12, 13, 14, 15, and 16) and thus indicate shallower settings than the Kimmeridgian coral-bearing limestones. In the context of generally low accommodation, low-amplitude and high-frequency sea-level fluctuations created significant bedding surfaces, whereas during the major transgression, such sea-level changes did not, or only indirectly, influence sedimentation (Strasser et al.

1999). These sedimentological considerations are consistent with a major highstand normal-regressive stage of relative sea-level evolution (Figs. 3, 4a). There is no discrete surface developed on top of the Kimmeridgian limestones that could qualify as maximum-flooding surface. Instead, the interval located at the boundary between the massive Kimmeridgian deposits and the well-bedded Tithonian-to-Berriasian strata is interpreted as a maximum-flooding zone (Figs. 3, 4a). The observed transgressive–regressive trend of relative sea-level change with the turn-around towards the end of the Kimmeridgian has been documented also in other European basins and corresponds to a major transgressive–regressive cycle of Hardenbol et al. (1998) (Fig. 2).

Sequence boundaries in peritidal carbonates

In platform carbonates, one of the unequivocal sedimentary expressions of relative sea-level fall that are usually chosen

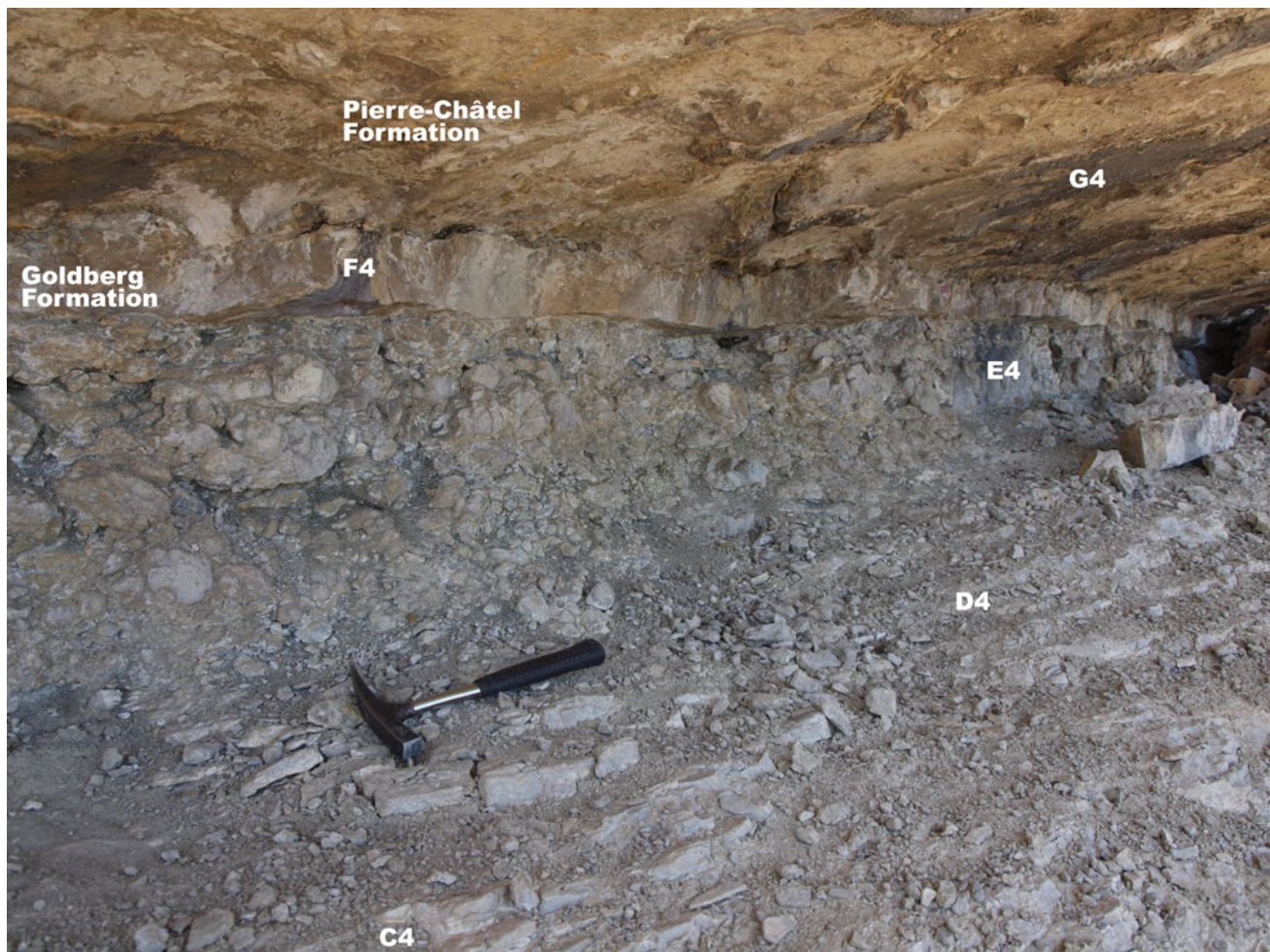


Fig. 12 Outcrop photograph of the strata surrounding sequence boundary Be4. Note the presence of a laterally continuous decimetre-thick breccia. C4 to G4 labels correspond to beds referred to in the text and indicated in Fig. 11

as sequence boundaries are karstified horizons (e.g., Van Buchem et al. 2002; Bernaus et al. 2003; Bover-Arnal et al. 2011). In this regard, no evidence of karstification was recognized in the studied sedimentary succession of Mount Salève. Nevertheless, the Berriasian strata examined above and below the sequence boundaries Be1, Be2, Be4, and Be8 of Strasser and Hillgärtner (1998) are formed by shallow subtidal deposits alternating with intertidal and/or supratidal lithofacies (Figs. 5, 6, 7, 8, 9, 10, 11, 12, 13, 14, 15, and 16), which manifest low accommodation when compared to the lithofacies exhibited by the underlying Kimmeridgian and Tithonian rocks.

When succeeding beds composed of intertidal and/or supratidal lithofacies are present and the different hierarchical levels of the surfaces bounding these strata cannot be established, it is difficult to attribute the sequence boundary to a specific bedding plane. In such cases, it is best to indicate a “sequence-boundary zone” (Montañez and Osleger 1993; Strasser et al. 1999), which defines a stratigraphic interval

comprising the shallowest facies and/or reflecting reduced depositional space.

Sequence-boundary zone Be1

Strasser and Hillgärtner (1998) placed sequence boundary Be1 at the top of the stratigraphic unit A1 (Fig. 5). This deposit is mainly formed by subtidal lithofacies, but the uppermost part exhibits keystone vugs, which are indicative of high-energy upper intertidal to lower supratidal beach settings (Dunham 1970). In addition, the bed is truncated by an erosive surface that is consistent with, but does not prove, subaerial exposure (Fig. 6). Thus, this surface constitutes a suitable option for a sequence boundary. However, above Be1, inter- and supra-tidal lithofacies (C1, E1 and F1) still occur intercalated between subtidal deposits (B1, D1 and G1). These peritidal lithofacies are characterized by algal-microbial laminites (Fig. 7b) typical of the upper part of a tidal flat (e.g., Shinn

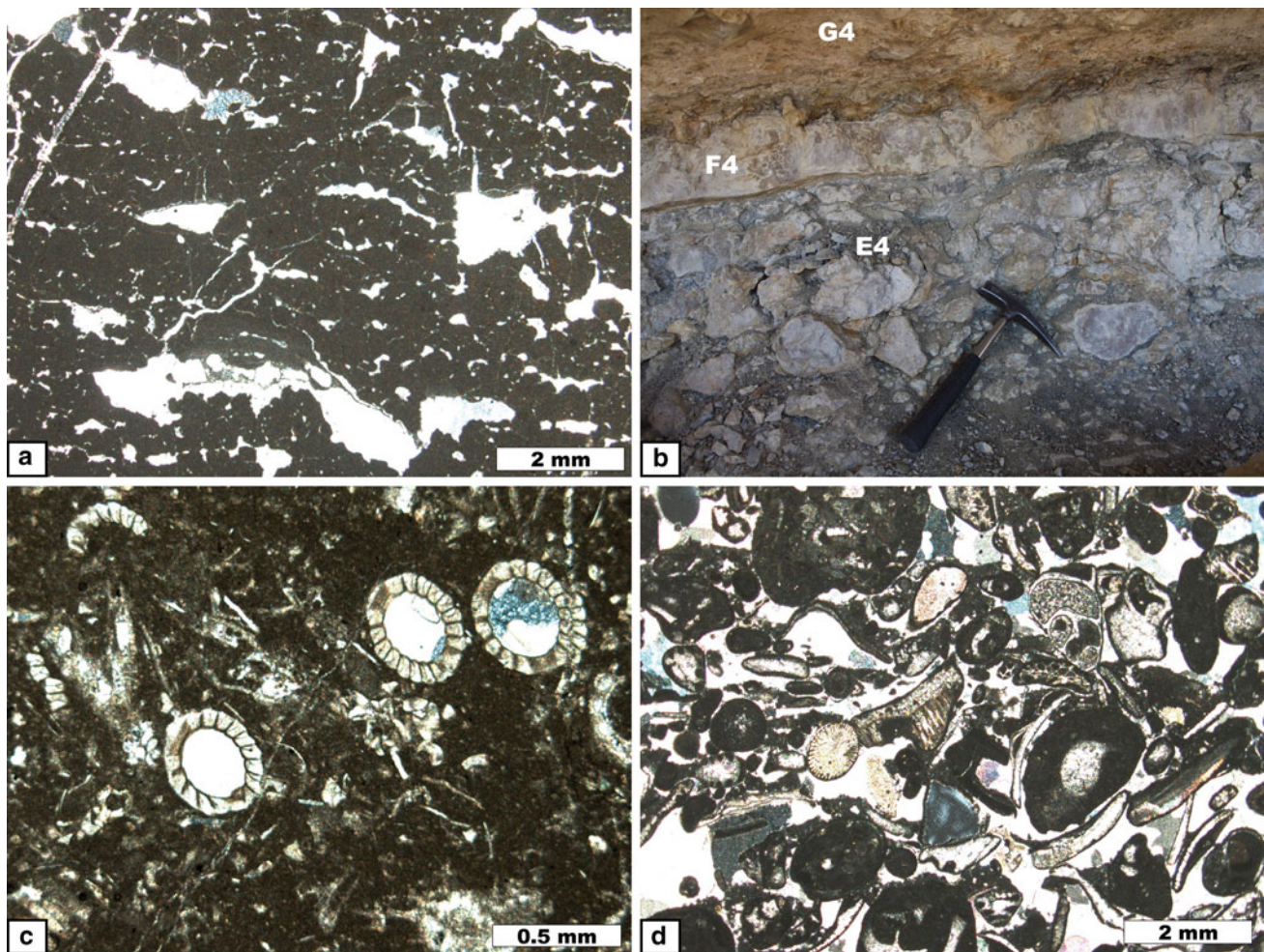


Fig. 13 Sedimentary facies around SB Be4. **a** Photomicrograph of characteristic fenestral porosity exhibited by the mudstones displaying desiccation polygons in the uppermost Goldberg Formation, bed D4. **b** Detail of the breccia/conglomerate deposit (E4). F4 and G4 correspond to a brackish-water wackestone and a fully marine

grainstone deposit, respectively; hammer = 32 cm. **c** Microfacies of porocharacean remains showing sections of gyrogonites and thalli, bed F4. **d** Photomicrograph of moderately sorted peloidal-skeletal grainstone texture typical of the base of the Pierre-Châtel Formation, bed G4

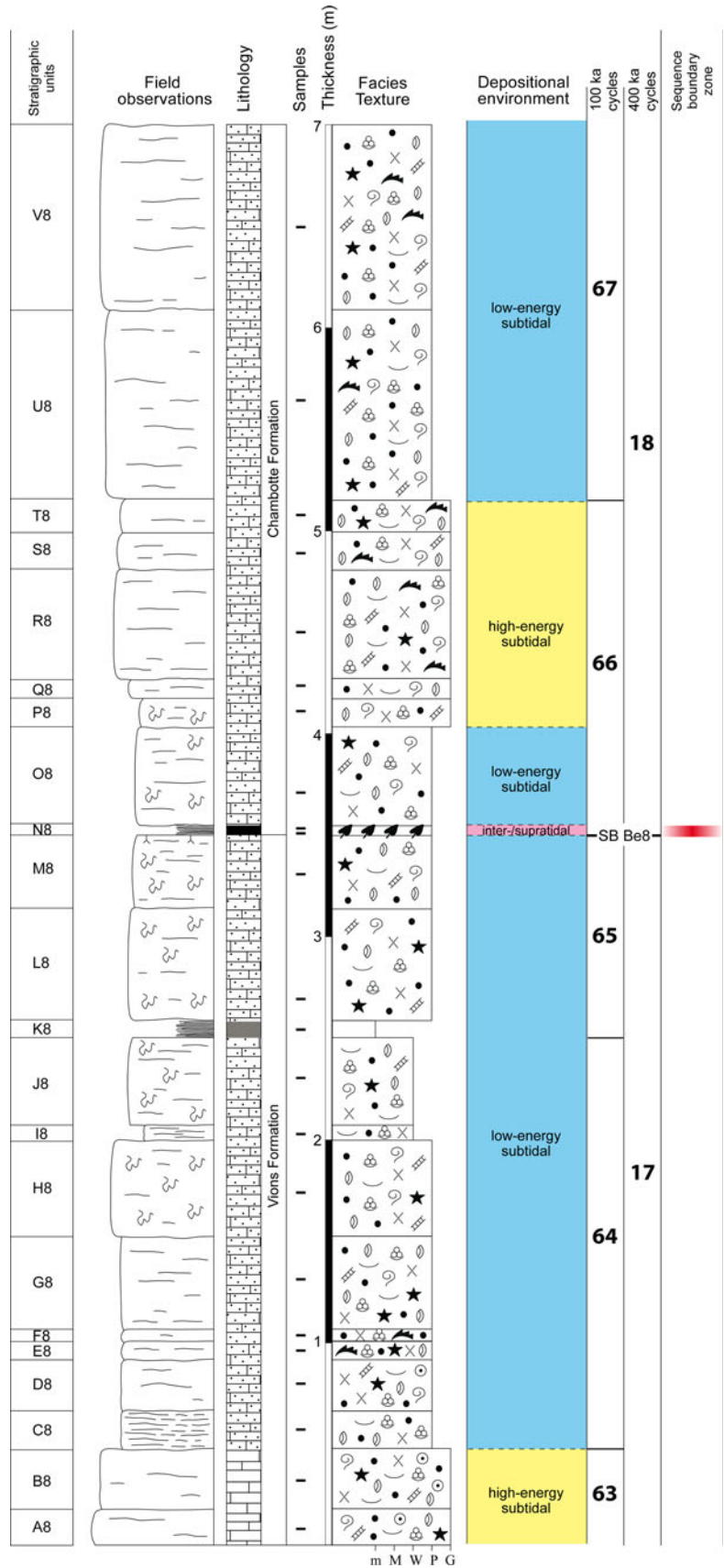
et al. 1969) and by homogeneous populations of porocharaceans (Fig. 7f), which commonly developed in brackish-water ponds or marshes (e.g., Climent-Domènech et al. 2009). These low-energy inter- to supratidal deposits certainly were accumulated in more proximal settings than the high-energy grainstone (A1; Fig. 7a) with keystone vugs. Moreover, the strata overlying the top of A1 display a thickening–thinning trend in the following 4 m (B1–G1), suggesting that accommodation increased then decreased after the formation of the erosional surface Be1 (Fig. 5). The overlying stratigraphic unit H1 is 8 m thick and marks a significant gain of depositional space. It also contains fully marine subtidal facies and thus formed during relative sea-level rise. Therefore, the sequence boundary Be1 would be best represented by a sequence-boundary zone comprising the uppermost part of stratigraphic unit A1 and

units B1 to F1 (Figs. 5, 6). Strasser and Hillgärtner (1998) interpreted the interval covered by units B1 to F1 as having formed by two sea-level cycles in tune with the 100-kyr orbital eccentricity cycle. These higher-frequency sea-level changes were superimposed onto the lower-frequency trend that was responsible for the sequence-boundary interval with low accommodation. Nevertheless, some accommodation had to be available to record the observed sequences, but carbonate accumulation was high enough to maintain the sediment surface in the intertidal or supratidal zone.

Sequence-boundary zone Be2

Sequence boundary Be2 was placed by Strasser and Hillgärtner (1998) at the top of mudstone deposits exhibiting

Fig. 14 Measured log and interpretation of the stratigraphic interval surrounding sequence boundary Be 8. See Fig. 5 for legend. Cyclostratigraphic interpretation according to Strasser and Hillgärtner (1998)



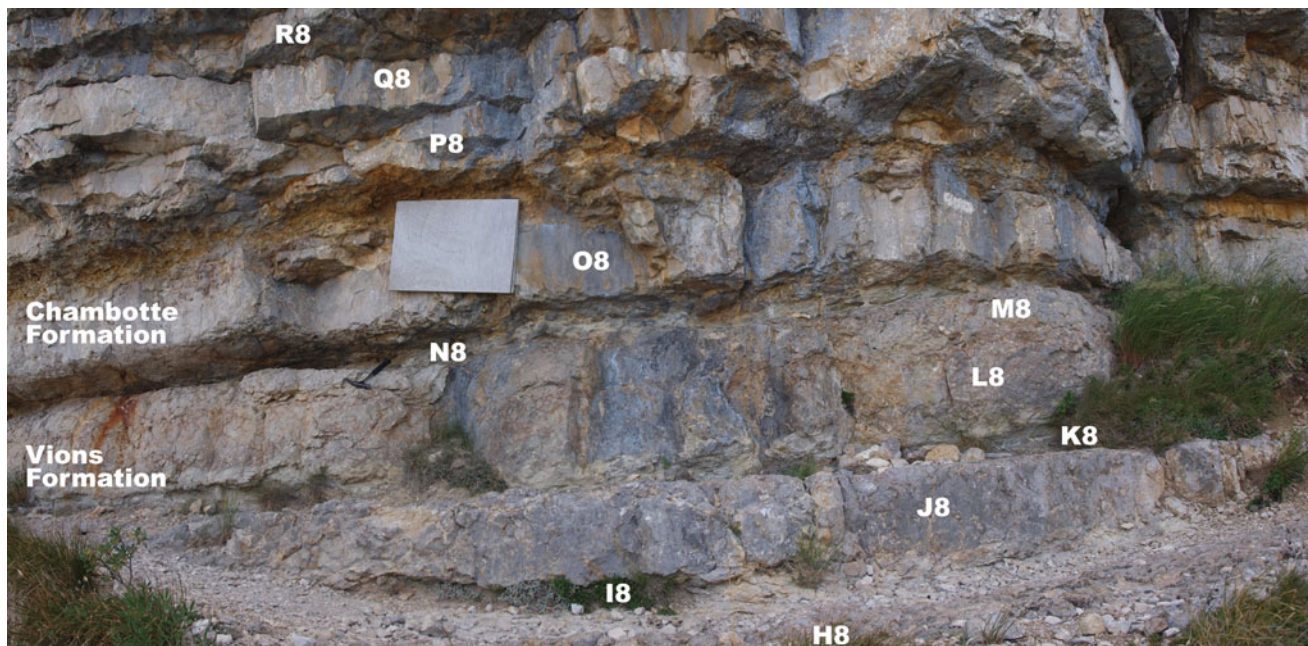


Fig. 15 Outcrop photograph of the strata surrounding SB Be8. This boundary also marks the limit between the Vions and Chambotte formations. Note how the beds are laterally continuous. H8 to R8

labels correspond to beds referred to in the text and indicated in Fig. 14. White panel is a station of a didactic geological trail; hammer = 32 cm

desiccation polygons (E2; Figs. 8, 10a), which are characteristic of the upper transitional part of the intertidal flat (e.g., Hardie 1977). Given that these layers with mud-cracked surfaces (D2–E2) are stratigraphically above low-energy subtidal wackestones (A2–C2), they do mark a shallowing-up. This could have been achieved by simple filling in of depositional space but could also have been forced by a slight drop in relative sea level. Accommodation had to be created again to form the ooid shoals represented by unit G2 (Fig. 8), which were cemented as beachrock and covered by calcrete (H2; Fig. 10e) during a subsequent relative sea-level drop. The fact that at least three different lithologies occur within the breccia/conglomerate (I2; Figs. 9, 10e) implies that these sediments must have accumulated, then lithified, and were reworked during one or several sea-level cycles (one bed may contain several lithologies, or several beds can have the same lithology). Accommodation in this case was not enough to record individual beds but only the products of dismantling and reworking. This scenario is repeated once more to form units L2 and M2 (Figs. 9, 10f), albeit with less reworking since the clasts in M2 correspond to the underlying facies. Strasser and Hillgärtner (1998) proposed that the interval between units F2 and M2 corresponds to two (100 kyr) sea-level cycles. Hence, a sequence-boundary zone including the stratigraphic units D2–M2 (Figs. 8, 9) would be more appropriate to describe this interval of generally low accommodation than a single sequence-boundary surface. The stratigraphic units N2 and O2 mark the start of the

transgression above the sequence-boundary zone, given that they display an increased thickness and, thus, a gain of accommodation with respect to the succession below (Fig. 8).

Sequence-boundary zone Be4

Following the same criteria as for sequence boundary Be2, Strasser and Hillgärtner (1998) positioned sequence boundary Be4 surmounting inter- to supra-tidal algal-microbial mat deposits with desiccation cracks and birds-eyes (C4–D4; Figs. 11, 13a). Above this surface, however, a breccia/conglomerate (E4; Fig. 13b) indicating a high-energy inter- to supra-tidal beach zone (e.g., El-Sayed 1999; Stephenson and Naylor 2011) and a layer containing monospecific populations of poracharaceans (F4; Fig. 13c) typical of brackish marsh environments (e.g., Climent-Domènech et al. 2009) imply that the marine regression continued throughout the stratigraphic units E4–F4. Consequently, the sequence boundary would be best characterized by a zone including the beds C4–F4 (Figs. 11, 12). The metric thickness of the cross-bedded grainstone G4 indicates that the gain of depositional space linked to the subsequent transgressive pulse occurred above the sequence-boundary zone. The upward passage from inter-/supratidal (F4) to subtidal (G4) lithofacies is in agreement with this reasoning (Fig. 11). According to the interpretation of Strasser and Hillgärtner (1998), 400 kyr are comprised in unit E4. This corresponds to the hiatus between

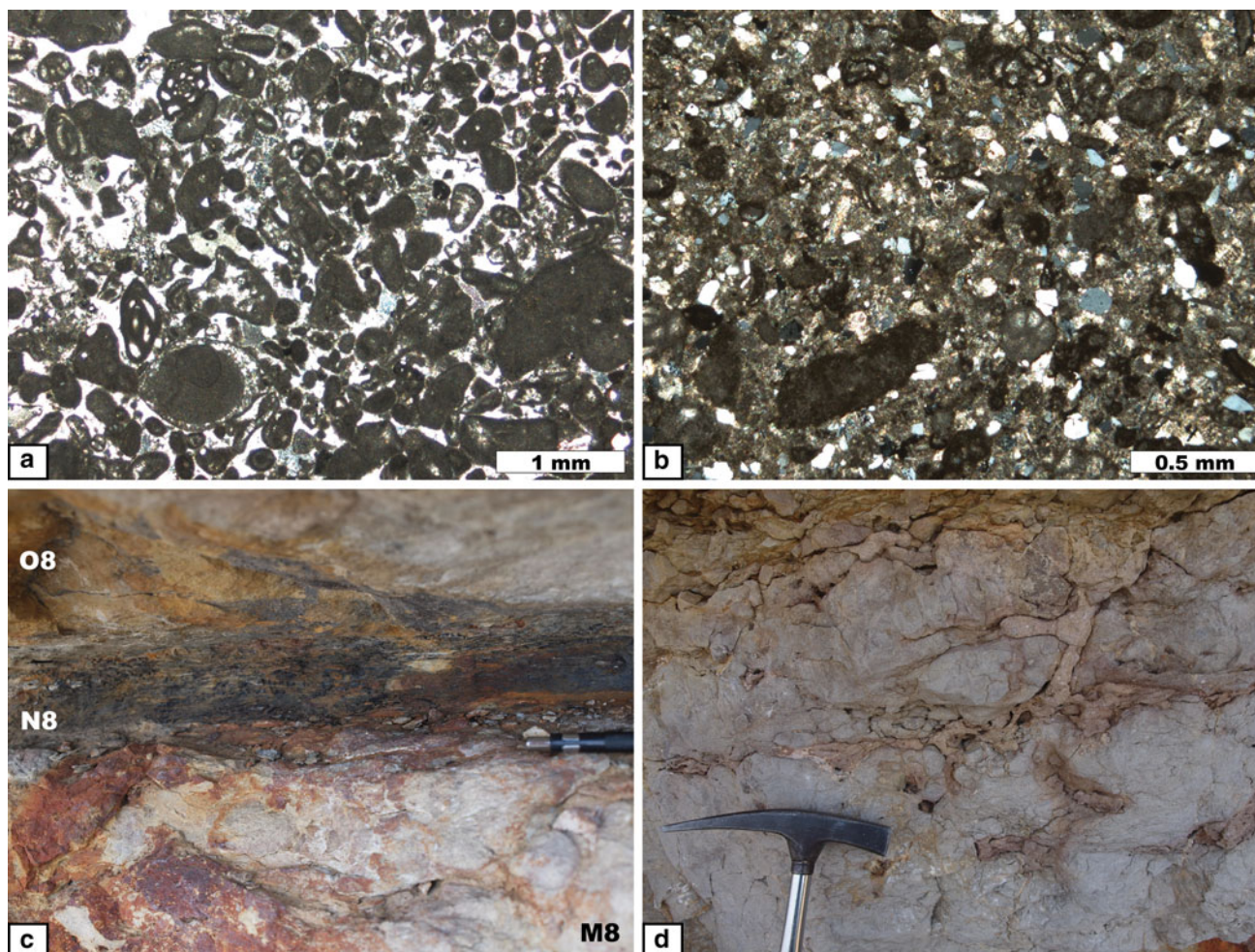


Fig. 16 Sedimentary facies around SB Be8. **a** Photomicrograph of moderately sorted peloidal-skeletal grainstone in the upper part of the Vions Formation, bed A8. **b** Photomicrograph of siliciclastic-influenced lithofacies characteristic of the uppermost part of the Vions Formation, bed L8. Note abundant angular to subrounded quartz grains. **c** Close-up view of the coal horizon (N8). M8 and O8

correspond to burrowed limestones with a packstone texture that belong respectively to the top of the Vions and to the base of the Chambotte formations (see Figs. 14, 15). The reddish colour displayed by bed M8 is the result of iron impregnation; visible part of pen = 4.2 cm. **d** Detail of *Thalassinoides* burrows preserved in bed O8; visible part of hammer = 11 cm

the Goldberg and the Pierre-Châtel formations evidenced by biostratigraphy (Clavel et al. 1986) and indicated in Fig. 2.

Sequence-boundary zone Be8

Sequence boundary Be8 was placed by Strasser and Hillgärtner (1998) at the base of the clayey coal level (N8; Figs. 14, 15, and 16c), which crops out in the uppermost part of the Berriasian succession. In carbonate platform environments, coal typically accumulates in brackish to fully marine swamps developed on the tidal flat (e.g., Shao et al. 1998). Given that subtidal deposits, thus deeper lithofacies, characterize the strata above and below this coal-bearing horizon, the base of this inter- to supratidal level constitutes a good candidate for a sequence boundary. Consistently, this surface exhibits scarce root traces

(Fig. 14). Nevertheless, the latter surface cannot be followed basinwards, and therefore, it is not possible to discriminate whether or not it was generated during the lowest point of relative sea-level. In siliciclastic coastal systems, coals are commonly interpreted to be formed and preserved during transgression (e.g., Coe et al. 2003). However, the coal horizon observed at Salève is only 2–3 cm thick and disappears laterally. Such a reduced deposit could have also formed during a lowstand stage of relative sea-level and was preserved during a high-frequency transgressive pulse superimposed on the long-term sea-level fall. In this respect, the lowest point of long-term relative sea level could also be located within or at the top of the coal layer. Then, the base of the coal accumulation would correspond to a basal surface of forced regression sensu Hunt and Tucker (1992). Given that the sequence-stratigraphic significance and hierarchy of the different surfaces cannot be

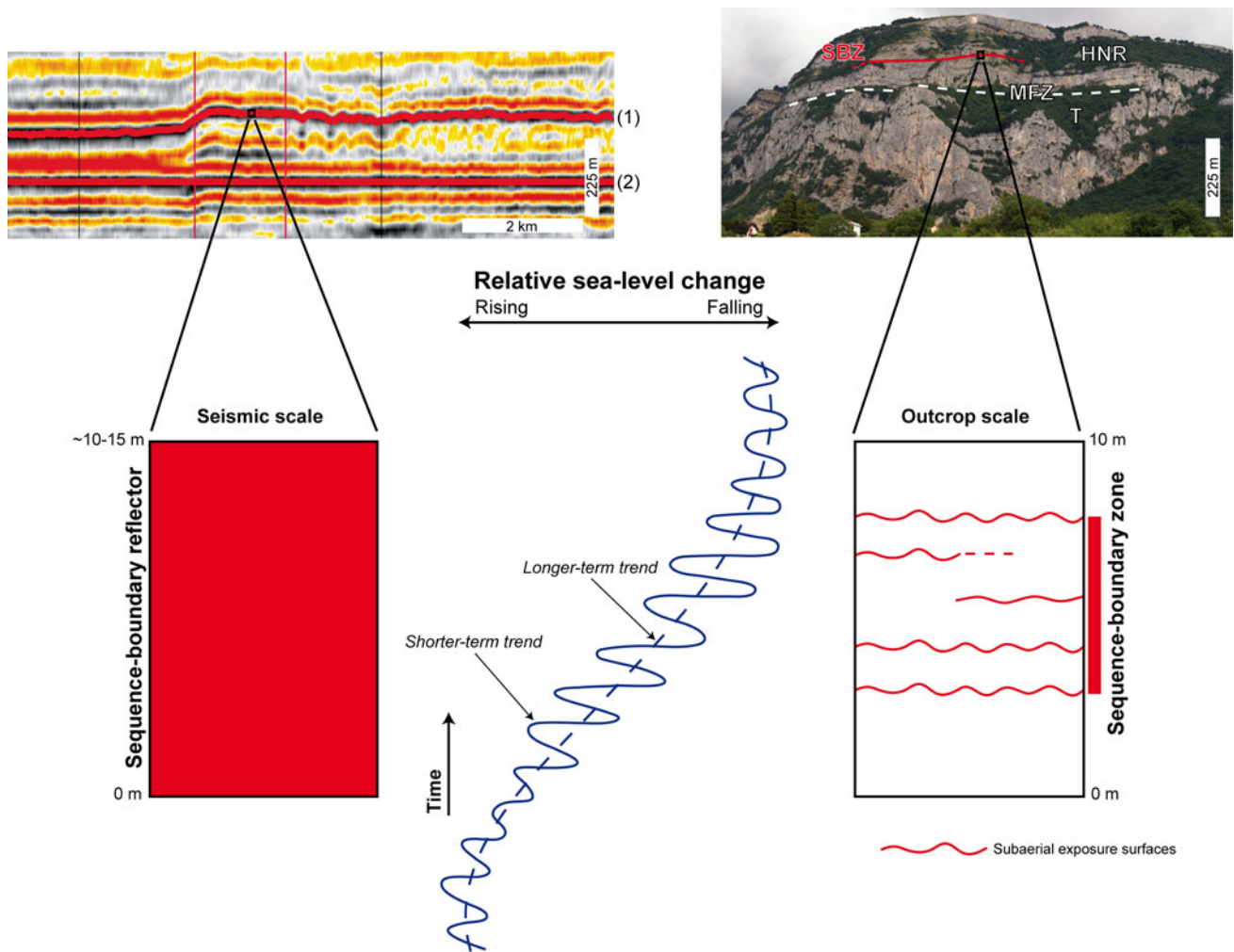


Fig. 17 Conceptual figure comparing a sequence-boundary reflector mapped on seismic data with an outcropping sequence-boundary zone. Note that a sequence-boundary reflector when seen in outcrop may present several subaerial exposure surfaces and, thus, several candidate surfaces for a sequence boundary. The sequence-boundary zone was structured by high-frequency sea-level fluctuations, whereas the sequence-boundary reflector only records a relative sea-level fall of the longer-term trend. The seismic cross section is taken from Yose et al. (2010) and shows highstand aggrading platform carbonates of the Shu’aiba Formation (Aptian) from onshore Abu Dhabi (UAE).

Reflector 1 marks the top of the Shu’aiba Formation, which corresponds to a regional sequence boundary related to subaerial exposure. This surface also corresponds to the top of the Shu’aiba reservoir, which is sealed by the shales of the Nahr Umr Formation (Albian). Reflector 2 marks the base of the Shu’aiba reservoir. The field view corresponds to the Late Jurassic–Early Cretaceous succession of Mount Salève shown in Fig. 4a. *SBZ* sequence-boundary zone, *HNR* highstand normal-regressive deposits, *T* transgressive deposits, *MFZ* maximum-flooding zone

determined, in this last case study, a zone covering the entire coal-bearing horizon would best represent the sequence boundary (Fig. 14).

The making of sequence boundaries

The sequence-boundary zones discussed here (Figs. 5, 8, 11, and 14) provide stratigraphic windows illustrating the sedimentary response of carbonate platforms to forced regressive and lowstand normal-regressive stages of relative sea-level change. To determine the origin of relative sea-level fluctuations in carbonate sedimentary successions is always a difficult task and not free of controversies.

Above all, in outcrops of reduced lateral extension where a perspective of the basin-wide stratigraphic evolution is lacking, assumptions are unavoidable. Numerous natural processes could have acted, either in isolation or combined, to generate the long-term lowering stages of relative sea level recognized in the geological record analysed. These potential mechanisms are summarized in Immenhauser (2005) and mainly include glacio-eustasy, tectono-eustasy, and thermo-eustasy.

According to Strasser and Hillgärtner (1998), the Berriasian sequence boundaries of Mount Salève can be explained as corresponding to Tethyan long-term (third-order) relative sea-level falls (Hardenbol et al. 1998). Recently, Boulila

et al. (2011) have concluded that most of the Mesozoic third-order sea-level changes reported worldwide seem to be linked to long-period astronomical cycles.

The long-term regressive phases recognized are overprinted by a higher-frequency evolution of relative sea level. The stratigraphic packaging within the sequence-boundary zones has been regarded mainly as the result of orbitally controlled amplitude changes in eustatic sea level, which were to some extent distorted by synsedimentary tectonics (Strasser 1988, 1994; Strasser and Hillgärtner 1998). In addition, autocyclic processes such as variations in the rates of carbonate production and accumulation or the lateral migration of peritidal facies belts (e.g., Hardie 1977; Pratt and James 1986) certainly have also played a part in the formation of the stratigraphic record. Accordingly, to link the lithofacies evolution observed to determined shifts in the amplitude of relative sea-level change is not free of uncertainties, especially if the degree of completeness of the stratigraphic record is not known. Nevertheless, some aspects concerning the making of the sequence-boundary zones can indeed be considered.

The sequence-boundary zones containing stratigraphic surfaces Be2 and Be4 (Figs. 8, 11) are characterized by the presence of reworked, previously lithified sediments, which are absent in Be1 and Be8. These breccia/conglomerate horizons (Figs. 8, 9, 11, and 12) highlight the importance of reworking processes in peritidal zones (e.g., Wright 1984; Strasser and Davaud 1986). Commonly such intraclasts are transported to foreshore and backshore environments during storm events, although detached beachrock slabs may slide into the shallow subtidal realm as well. The breccia/conglomerate deposits contain cobble- to boulder-sized clasts exhibiting distinct microfacies. These lithoclasts constitute the only records of completely dismantled depositional sequences, which were not preserved in the section logged but may be still recognizable in nearby exposures (Strasser 1994).

The preservation of these breccia/conglomerate levels, which are indicative of ancient high-energy intertidal settings, is exceptional because high-energy intertidal zones are very limited in extent in comparison to the supratidal, subtidal, and low-energy intertidal zones. It is also exceptional to find them preserved in a vertical sedimentary succession. If such a small depositional area persists in several stratigraphic levels in the same geographical position, this indicates that the sedimentary system was relatively stable and did not suffer significant shifts of facies belts (retrogradation or progradation). Therefore, rates of carbonate production and accumulation, higher-frequency sea-level changes, and subsidence during the time interval comprised between sequence-boundary zones Be2 and Be4 may have been controlled by similar, recurrent patterns (also sequence-boundary zone Be3, not documented in the

present study, exhibits a breccia/conglomerate level; Strasser and Hillgärtner 1998). Aggradational sedimentary systems are typical of early stages of highstand normal regression (Neal and Abreu 2009; Catuneanu et al. 2009). Hence, these observations would be in accordance with the large-scale sequence-stratigraphic framework proposed herein (Figs. 3, 4a).

The imprint of climate on the sequence-boundary zones interpreted is also noticeable. Sequence-boundary zone Be8 is constituted by a coal level (Figs. 14, 16c), which is overlain and underlain by strata containing abundant quartz grains (Figs. 14, 16b). The marls preserved in this stratigraphic interval are rich in kaolinite (Hillgärtner 1999) that is commonly formed in palaeosoils developed under humid conditions (e.g., Curtis 1990). Coal deposits represent the preservation in shallow, oxygen-poor waters of vegetation that flourished in a humid climate (e.g., Parrish et al. 1982). Together, these sedimentary features indicate that this stratigraphic interval was formed under a humid climate (Fig. 2). The sudden appearance of siliciclastics in this Berriasian carbonate succession (Fig. 14) is symptomatic of uplift processes, with additional intensified continental weathering and runoff rates linked to an accelerated hydrological cycle (e.g., Leeder et al. 1998). The iron that gives the reddish stain to the rock was washed into the system together with the siliciclastics.

On the other hand, sequence-boundary zones Be1, Be2, and Be4 (Figs. 5, 8, and 11) lack evidence of siliciclastic input and contain algal-microbial mat deposits (Figs. 7b, 13a), which exhibit desiccation cracks (Fig. 10a) and, in the case of sequence-boundary zone Be1, are partly dolomitized. Algal-microbial mat deposits with mud cracks are common in modern tidal flat environments developed in arid to semiarid areas (e.g., Alsharhan and Kendall 2003). The sequence-boundary zone Be2 includes a calcrete crust (Figs. 8, 10e). Calcretes are mainly formed in semi-arid to arid environments (Scholle and Ulmer-Scholle 2003). Therefore, these sedimentary peculiarities coupled with the absence of terrigenous grains indicate a more arid climate (Fig. 2). In addition, the marly levels preserved in these stratigraphic intervals (Figs. 8, 11) contain green illite that formed by wetting and drying in the intertidal zone (Deconinck and Strasser 1987). Higher abundances of illite with respect to kaolinite are commonly interpreted to reflect more arid climates (e.g., Ruffell et al. 2002). Pseudomorphs after gypsum and anhydrite have been found only in two levels between sequence-boundary zones Be2 and Be3, and the depositional environment there was interpreted as a sabkha (Strasser and Hillgärtner 1998). However, evaporite pseudomorphs are common in the Goldberg Formation in the Swiss Jura (Strasser 1988).

This climate change from more arid conditions (sequence-boundary zones Be1, Be2, and Be4) to a more

humid climate (sequence-boundary zone Be8) during the Late Berriasian (Fig. 2) has been recognized also in other coeval geological records from other basins in northern and western Europe (Price 1999; Ruffell et al. 2002). The aridity peak, however, occurred already in the Late Tithonian (Fig. 2; e.g., Rameil 2005). Superimposed on the general trend were high-frequency climate changes that led to an alternation of more arid and more humid conditions, as, for example, in the case of sequence-boundary zone Be1 where dolomitized microbial mats are overlain by brackish-water, charophyte-bearing limestones (Fig. 5).

A matter of scale

The thickness of the stratigraphic intervals comprising the sequence-boundary zones analysed is within or very close to the vertical resolution nowadays achieved in seismic profiles (5–15 m; e.g., Praeg 2003). Thus, the Berriasian intervals studied can be seen as outcrop examples of sequence-boundary reflectors mapped in subsurface successions of proximal platform carbonates. Whereas at seismic scale, only longer-term trends of relative sea-level change can be interpreted, in the outcrop the imprint of higher frequencies of relative sea-level change is potentially also discernible (Fig. 17). Especially, in peritidal successions, high-frequency relative sea-level fluctuations may structure the sedimentary record formed during longer-term regressive phases through successive surfaces of subaerial exposure, which can be grouped into a sequence-boundary zone (Figs. 5, 8, 11, 14, and 17). Therefore, a sequence-boundary reflector when expressed in outcrop is not necessarily a single surface but equivalent to a stratigraphic interval, which contains, depending on the sedimentary response to the high-frequency variations of relative sea level, a suite of features indicating loss of accommodation (Fig. 17).

Conclusions

The Late Jurassic (Kimmeridgian) to Early Cretaceous (Berriasian) platform carbonates of Mount Salève are excellent archives of the major climate and oceanographic changes that occurred during this time interval at the northern margin of the Alpine Tethys. These include (1) a major transgressive–regressive cycle of relative sea-level change, and (2) a climate shift from a more arid to more humid conditions from the Early to the Late Berriasian.

The major transgressive–regressive cycle is marked by Kimmeridgian transgressive coral-bearing limestones, which pass upwards to Tithonian–Berriasian normal-regressive peritidal deposits. The Kimmeridgian limestones are massive, seem to be stacked in an aggrading fashion,

and constitute a carbonate system that kept pace with relative sea-level rise. The Tithonian-to-Berriasian deposits reflect a reduced accommodation and correspond to well-bedded peritidal carbonates. The vertical persistence of upper intertidal to lower supratidal lithofacies throughout the Early Berriasian succession is indicative of an aggradational carbonate system. This is consistent with an early stage of a highstand phase of relative sea level.

The climate change is evidenced by the absence of siliciclastic grains and the presence of sedimentary features such as algal-microbial laminites with desiccation cracks and a calcrete crust in the Early Berriasian stratigraphic intervals analysed, and by the occurrence of abundant detrital quartz and of a coal horizon in the Late Berriasian sedimentary succession. Higher abundance of illite with respect to kaolinite in the Early Berriasian marly intervals, and the higher dominance of kaolinite with respect to illite in the Late Berriasian marl deposits are in accordance with this long-term climatic change.

The four sequence-boundary zones analysed comprise more than one candidate for a sequence boundary and thus demonstrate that higher-frequency sea-level changes, superposed to the major regressive context, structured this highstand phase. Depending on local sedimentological conditions and on the predominating climate, each sequence-boundary zone developed its own specific features.

The thicknesses of the studied stratigraphic intervals comprising sequence-boundary zones are comparable to the vertical resolution of sequence-boundary reflectors from high-resolution seismic data. Therefore, the detailed stratigraphic logs shown in this study can be regarded as exemplary outcrop analogues of sequence-boundary reflectors mapped in subsurface peritidal carbonate successions.

Acknowledgments We are grateful to Dan Bosence, Marc Aurell, and an anonymous reviewer for their careful reviews and constructive suggestions. Felix Schlagintweit and Carles Martín-Closas are thanked for having determined several fossil specimens. David Jaramillo-Vogel is acknowledged for fruitful discussions on the ideas presented in this paper. We would like to thank Lyndon A. Yose for providing information on the seismic transect from onshore Abu Dhabi shown in this paper. Financial support for this research was provided by the Swiss National Science Foundation grants no. 20-121545 and 20-137568.

References

- Alsharhan AS, Kendall CGStC (2003) Holocene coastal carbonates and evaporites of the southern Arabian Gulf and their ancient analogues. *Earth Sci Rev* 61:191–243
- Aurell M, Bádenas B (2004) Facies and depositional sequence evolution controlled by high-frequency sea-level changes in a shallow-water carbonate ramp (late Kimmeridgian, NE Spain). *Geol Mag* 141:717–733
- Bádenas B, Aurell M, Salas R (2004) Three orders of regional sea-level changes control facies and stacking patterns of shallow

- platform carbonates in the Maestrat Basin (Tithonian-Berriasian, NE Spain). *Int J Earth Sci* 93:144–162
- Bernaus JM, Arnaud-Vanneau A, Caus E (2003) Carbonate platform sequence stratigraphy in a rapidly subsiding area: the Late Barremian-Early Aptian of the Organyà basin, Spanish Pyrenees. *Sed Geol* 159:177–201
- Bernier P (1984) Les formations carbonatées du Kimméridgien et du Portlandien dans le Jura méridional. *Stratigraphie, micropaléontologie et sédimentologie*. Doc Lab Géol Lyon 92, 803 pp
- Booler J, Tucker ME (2002) Distribution and geometry of facies and early diagenesis: the key to accommodation space variation and sequence stratigraphy: Upper Cretaceous Congost Carbonate platform, Spanish Pyrenees. *Sed Geol* 146:225–247
- Borgomano JRF (2000) The Upper Cretaceous carbonates of the Gargano-Murge region, southern Italy: a model of platform-to-basin transition. *AAPG Bull* 84:1561–1588
- Boulila S, Galbrun B, Miller KG, Pekar SF, Browning JV, Laskar J, Wright JD (2011) On the origin of Cenozoic and Mesozoic “third-order” eustatic sequences. *Earth Sci Rev* 109:94–112
- Bover-Amal T, Salas R, Moreno-Bedmar JA, Bitzer K (2009) Sequence stratigraphy and architecture of a late early–Middle Aptian carbonate platform succession from the western Maestrat Basin (Iberian Chain, Spain). *Sed Geol* 219:280–301
- Bover-Amal T, Moreno-Bedmar JA, Salas R, Skelton PW, Bitzer K, Gili E (2010) Sedimentary evolution of an Aptian syn-rift carbonate system (Maestrat Basin, E Spain): effects of accommodation and environmental change. *Geol Acta* 8:249–280
- Bover-Amal T, Jaramillo-Vogel D, Showani A, Strasser A (2011) Late Eocene transgressive sedimentation in the western Swiss Alps: records of autochthonous and quasi-autochthonous biofacies on a karstic rocky shore. *Palaeogeogr Palaeoclimatol Palaeoecol* 312:24–39
- Carozzi AV (1955) Sédimentation récifale rythmique dans le Jurassique supérieur du Grand-Salève. *Geol Rundsch* 43:433–446
- Catuneanu O, Abreu V, Bhattacharya JP, Blum MD, Dalrymple RW, Eriksson PG, Fielding CR, Fisher WL, Galloway WE, Gibling MR, Giles KA, Holbrook JM, Jordan R, Kendall CGStC, Macurda B, Martinsen OJ, Miall AD, Neal JE, Nummedal D, Pomar L, Posamentier HW, Pratt BR, Sarg JF, Shanley KW, Steel RJ, Strasser A, Tucker ME, Winker C (2009) Towards the standardization of sequence stratigraphy. *Earth Sci Rev* 92:1–33
- Clavel B, Charollais J, Busnardo R, Le Hégarat G (1986) Précisions stratigraphiques sur le Crétacé inférieur basal du Jura méridional. *Eclogae Geol Helv* 79:319–341
- Climent-Domènech H, Martín-Closas C, Salas R (2009) Charophyte-rich microfacies in the Barremian of the Eastern Iberian Chain (Spain). *Facies* 55:387–400
- Coe AL, Bosence DWJ, Church KD, Flint SS, Howell JA, Wilson RCL (2003) The sedimentary record of sea-level change. Cambridge University Press and The Open University, Cambridge, p 288
- Colombié C, Rameil N (2007) Tethyan-to-boreal correlation in the Kimmeridgian using high-resolution sequence stratigraphy (Vocontian Basin, Swiss Jura, Boulonnais, Dorset). *Int J Earth Sci* 96:567–591
- Colombié C, Strasser A (2005) Facies, cycles, and controls on the evolution of a keep-up carbonate platform (Kimmeridgian, Swiss Jura). *Sedimentology* 52:1207–1227
- Curtis CD (1990) Aspects of climatic influence on the clay mineralogy and geochemistry of soils, paleosols and clastic sedimentary rocks. *J Geol Soc London* 147:351–357
- de Saussure H-B (1779–1796) Voyages dans les Alpes précédés d'un essai sur l'histoire naturelle des environs de Genève. Fauche-Borel, Neuchâtel, 4 vols
- Deconinck J-F, Strasser A (1987) Sedimentology, clay mineralogy and depositional environment of Purbeckian green marls (Swiss and French Jura). *Eclogae Geol Helv* 80:753–772
- Deville Q (1990) Chronostratigraphie et lithostratigraphie synthétique du Jurassique supérieur et du Crétacé inférieur de la partie méridionale du Grand Salève (Haute Savoie, France). *Archs Sci Genève* 31:215–235
- Deville Q (1991) Stratigraphie, sédimentologie et environnements de dépôts, et analyse séquentielle dans les terrains entre le Kimméridgien supérieur et le Valanginian du Mont-Salève (Haute Savoie, France). PhD thesis, Université de Genève, 141 pp
- Dunham RJ (1962) Classification of carbonate rocks according to depositional texture. In: Ham WE (ed) *Classification of carbonate rocks*. AAPG Mem 1:108–121
- Dunham RJ (1970) Keystone vugs in carbonate beach deposits. *Am Assoc Pet Geol Bull* 54:845
- El-Sayed MI (1999) Tidal flat rocks and sediments along the eastern coast of the United Arab Emirates. *Carbonates Evaporites* 14:106–120
- Enay R (1965) Les formations coralliennes de Saint-Germain-de-Joux (Ain). *Bull Soc Géol France* 7:23–31
- Gorin GE, Signer C, Amberger G (1993) Structural configuration of the western Swiss Molasse Basin as defined by reflection seismic data. *Eclogae Geol Helv* 86:693–716
- Gourrat C, Masse J-P, Skelton PW (2003) *Hypelasma salevensis* (FAVRE, 1913) from the Upper Kimmeridgian of the French Jura, and the origin of the Rudist Family Requiieniidae. *Geol Croat* 56:139–148
- Gradstein FM, Ogg JG, Smith AG (2004) *A geologic time scale 2004*. Cambridge University Press, Cambridge
- Häfeli C (1966) Die Jura/Kreide-Grenzsichten im Bielerseegebiet (Kt. Bern). *Eclogae Geol Helv* 59:565–696
- Hardenbol J, Thierry J, Farley MB, Jacquin T, de Graciansky PC, Vail PR (1998) Mesozoic and Cenozoic sequence chronostratigraphic framework of European basins. In: Graciansky PC, Hardenbol J, Jacquin T, Vail PR (eds) *Mesozoic and Cenozoic sequence stratigraphy of European Basins*. SEPM Spec Publ 60:3–13, charts 1–8
- Hardie LA (1977) Sedimentation on the modern carbonate tidal flats of northwest Andros Island, Bahamas. The Johns Hopkins University Press, Baltimore
- Hillgärtner H (1998) Discontinuity surfaces on a shallow-marine carbonate platform (Berriasian, Valanginian, France and Switzerland). *J Sediment Res* 68:1093–1108
- Hillgärtner H (1999) The evolution of the French Jura platform during the Late Berriasian to Early Valanginian: controlling factors and timing. *GeoFocus* 1:203
- Hillgärtner H, Strasser A (2003) Quantification of high-frequency sea-level fluctuations in shallow-water carbonates: an example from the Berriasian-Valanginian (French Jura). *Palaeogeogr Palaeoclimatol Palaeoecol* 200:43–63
- Hunt D, Tucker ME (1992) Stranded parasequences and the forced regressive wedge systems tract: deposition during base-level fall. *Sed Geol* 81:1–9
- Immenhauser A (2005) High-rate sea-level change during the Mesozoic: new approaches to an old problem. *Sed Geol* 175:277–296
- James NP (1972) Holocene and Pleistocene calcareous crust (caliche) profiles: criteria for subaerial exposure. *J Sediment Petrol* 42:817–836
- Joukowsky E, Favre J (1913) *Monographie géologique et paléontologique du Salève* (Haute Savoie, France). Mém Soc Phys et Hist Nat Genève 37:295–523
- Le Hégarat G, Remane J (1968) Tithonique supérieur et Berriasien de l'Ardèche et de l'Hérault: corrélation des ammonites et des calpionelles. *Géobios* 1:7–70
- Leeder MR, Harris T, Kirkby MJ (1998) Sediment supply and climate change: implications for basin stratigraphy. *Basin Res* 10:7–18

- Lombard A (1967) Le Salève. In: Guide géologique de la Suisse 2:54–57
- Mojon P-O (1988) Contribution à l'étude micropaléontologique, paléocéologique et biostratigraphique des faciès "portlandiens" et "purbeckiens" (limite Jurassique-Crétacé) du Salève (Haute-Savoie, France). *Arch Sci Genève* 41:99–102
- Montañez IP, Osleger DA (1993) Parasequence stacking patterns, third-order accommodation events, and sequence stratigraphy of Middle to Upper Cambrian platform carbonates, Bonanza King Formation, southern Great Basin. In: Loucks RG, Sarg JF (eds) Carbonate sequence stratigraphy. AAPG Mem 57:305–326
- Neal J, Abreu V (2009) Sequence stratigraphy hierarchy and the accommodation succession method. *Geology* 37:779–782
- Parrish JT, Ziegler AM, Scotese CR (1982) Rainfall patterns and the distribution of coals and evaporites in the Mesozoic and Cenozoic. *Palaeogeogr Palaeoclimatol Palaeoecol* 40:67–102
- Pasquier J-B, Strasser A (1997) Platform-to-basin correlation by high-resolution sequence stratigraphy and cyclostratigraphy (Berriasian, Switzerland and France). *Sedimentology* 44:1071–1092
- Praeg D (2003) Seismic imaging of mid-Pleistocene tunnel-valleys in the North Sea Basin—high resolution from low frequencies. *J Appl Geophys* 53:273–298
- Pratt BR, James NP (1986) The St George Group (Lower Ordovician) of western Newfoundland: tidal flat island model for carbonate sedimentation in shallow epeiric seas. *Sedimentology* 33:313–343
- Price GD (1999) The evidence and implications of polar ice during the Mesozoic. *Earth Sci Rev* 48:183–210
- Rameil N (2005) Carbonate sedimentology, sequence stratigraphy, and cyclostratigraphy of the Tithonian in the Swiss and French Jura Mountains. A high-resolution record of changes in sea level and climate. *GeoFocus* 13, 246 pp
- Robbin DM, Stipp JJ (1979) Depositional rate of laminated soilstone crust, Florida Keys. *J Sediment Petrol* 49:175–180
- Ruffell A, McKinley JM, Worden RH (2002) Comparison of clay mineral stratigraphy to other proxy palaeoclimate indicators in the Mesozoic of NW Europe. *Philos Trans R Soc Lond A* 360:675–693
- Scholle PA, Ulmer-Scholle DS (2003) A color guide to the petrography of carbonate rocks: grains, textures, porosity, diagenesis. AAPG Mem 77:459
- Shao L, Zhang P, Ren D, Lei J (1998) Late Permian coal-bearing carbonate successions in southern China: coal accumulation on carbonate platforms. *Int J Coal Geol* 37:235–256
- Shinn EA, Lloyd RM, Ginsburg RN (1969) Anatomy of a modern carbonate tidal-flat, Andros Island, Bahamas. *J Sediment Petrol* 39:1202–1228
- Signer C, Gorin GE (1995) New geological observations between the Jura and the Alps in the Geneva area, as derived from reflection seismic data. *Eclogae Geol Helv* 88:235–265
- Spence GH, Tucker ME (2007) A proposed integrated multi-signature model for peritidal cycles in carbonates. *J Sediment Res* 77:797–808
- Steinhauser N, Lombard A (1969) Définition de nouvelles unités lithostratigraphiques dans le Crétacé inférieur du Jura méridional (France). *C R Soc Phys Hist Nat Genève* 4:100–113
- Stephenson WJ, Naylor LA (2011) Geological controls on boulder production in a rock coast setting: insights from South Wales, UK. *Mar Geol* 283:12–24
- Strasser A (1988) Shallowing-upward sequences in Purbeckian peritidal carbonates (lowermost Cretaceous, Swiss and French Jura Mountains). *Sedimentology* 35:369–383
- Strasser A (1994) Lagoonal-peritidal carbonate cyclicity: French Jura Mountains. In: de Boer PL, Smith DG (eds) Orbital forcing and cyclic sequences. IAS Spec Publ 19:285–301
- Strasser A, Davaud E (1983) Black pebbles of the Purbeckian (Swiss and French Jura): lithology, geochemistry and origin. *Eclogae Geol Helv* 76:551–580
- Strasser A, Davaud E (1986) Formation of Holocene limestone sequences by progradation, cementation and erosion: two examples from the Bahamas. *J Sediment Petrol* 56:422–428
- Strasser A, Hillgärtner H (1998) High-frequency sea-level fluctuations recorded on a shallow carbonate platform (Berriasian and Lower Valanginian of Mount Salève, French Jura). *Eclogae Geol Helv* 91:375–390
- Strasser A, Davaud E, Jedoui Y (1989) Carbonate cements in Holocene beachrock: example from Bahiret el Biban, southeastern Tunisia. *Sed Geol* 62:89–100
- Strasser A, Pittet B, Hillgärtner H, Pasquier J-B (1999) Depositional sequences in shallow carbonate-dominated sedimentary systems: concepts for a high-resolution analysis. *Sed Geol* 128:201–221
- Strasser A, Hillgärtner H, Hug W, Pittet B (2000) Third-order depositional sequences reflecting Milankovitch cyclicity. *Terra Nova* 12:303–311
- Strasser A, Hillgärtner H, Pasquier J-B (2004) Cyclostratigraphic timing of sedimentary processes: an example from the Berriasian of the Swiss and French Jura Mountains. In: D'Argenio B, Fischer AG, Premoli Silva I, Weissert H, Ferreri V (eds) Cyclostratigraphy: approaches and case histories. SEPM Spec Publ 81:137–151
- Strasser A, Hilgen FJ, Heckel FH (2006) Cyclostratigraphy—concepts, definitions, and applications. *Newsl Stratigr* 42:75–114
- Van Buchem FSP, Razin P, Homewood PH, Oterdoom WH, Philip J (2002) Stratigraphic organisation of carbonate ramps and organic-rich intrashelf basins: the Natih Formation (Middle Cretaceous) of Northern Oman. AAPG Bull 86:21–53
- Wright VP (1984) Peritidal carbonate facies models: a review. *Geol J* 19:309–325
- Yose LA, Strohmenger CJ, Al-Hosani I, Bloch G, Al-Mehairi Y (2010) Sequence-stratigraphic evolution of an Aptian carbonate platform (Shu'aiba Formation), eastern Arabian Plate, onshore Abu Dhabi, United Arab Emirates. In: van Buchem FSP, Al-Husseini MI, Maurer F, Droste HJ (eds) Barremian—Aptian stratigraphy and hydrocarbon habitat of the eastern Arabian Plate. *GeoArabia Spec Publ* 4:309–340